# ULTRASONIC ABSORPTION IN AQUEOUS SUSPENSIONS OF SMALL ELASTIC PARTICLES

BY

STEPHEN ARTHUR HAWLEY
A.B., Knox College, 1961
M.S., University of Illinois, 1963

THESIS

Submitted in partial fulfillment of the requirements
for the degree of Doctor of Philosophy in Biophysics
in the Graduate College of the
University of Illinois, 1967

**Urbana, Illinois**

GRADUATE COLLEGE
330 ADMINISTRATION BUILDING

September 26, 1966

Dear Professor Dunn:

I understand that Stephen Arthur Hawley expects to complete his doctoral dissertation in the near future. As chairman of his doctoral committee, will you please be responsible for making the necessary arrangements concerning the time and place of the examination?

The final certificate, a deferred grade report form, and a card on which to notify the University Press of the examination have been sent to the departmental office. When the thesis has been accepted in final form, the certificate, signed by the committee, should be returned to the Graduate College together with a deferred grade report for the candidate's research credit. A copy of the printed Certificate of Approval, signed by the members of the committee and by the department head, must accompany each of the two copies of the thesis that are to be deposited with the Graduate College.

Very truly yours,

Stanton Millet

~~Stanton Millet~~
Associate Dean Raymond C. Williams

This committee is discharged as of January 31, 1967.

COMMITTEE

| | |
|---|---|
| Floyd Dunn ✓<br>Chairman | H. S. Ducoff (Biophysics) |
| K. E. Van Holde (Chem) | R. S. Wolfe (Micro) |
| F. J. Fry (Elect Engr) | cc: Professor B. C. Abbott |
| | |

UNIVERSITY OF ILLINOIS

Department of Physiology
and Biophysics
524 Burrill Hall
September 26, 1966

Dr. H. S. Ducoff
Dr. K. E. Van Holde
Dr. R. S. Wolfe
Dr. F. J. Fry

Dear Colleagues:

The final oral examination for Mr. Stephen A. Hawley will be held

Tuesday, September 27, 1966, at 3:00 p.m. in Room 526 Burrill Hall.

Sincerely,

Floyd Dunn
pcd

Floyd Dunn
Chairman

cc: Graduate College
Mr. S. A. Hawley
FD/ped

# ULTRASONIC ABSORPTION IN AQUEOUS SUSPENSIONS OF SMALL ELASTIC PARTICLES

Stephen Arthur Hawley, Ph.D.
Department of Biophysics
University of Illinois, 1967

The absorption of ultrasound has been measured in aqueous solutions of dextran, a quasi-linear anhydroglucose polymer, and in aqueous suspensions of small polystyrene particles over the frequency range 3 - 165 MHz. The absorption in dextran solutions has been found to be independent of molecular weight ( $10^4 \leq \overline{M}_w \leq 3.7 \times 10^5$ ) and substantially greater than would be anticipated from the dynamic shear viscosity contributions predicted on the basis of the Rouse theory. The absorption in aqueous polystyrene lattices has been measured in five suspensions with particle sizes ranging from 0.044 micron to 3.5 microns. Comparison of the absorption behavior to the Lamb-Urick-Epstein theory and to results obtained in bulk polystyrene reveal that neither relative motion nor internal viscosity of the particle contribute substantially to the observed acoustic attenuation. An Arrhenius dependence of absorption coefficient on temperature is observed in the lattices that indicates that dissipation of ultrasound is intimately associated with the liquid phase of the suspension. Comparison of the absorption properties of the lattices to that observed to that found in solutions of bovine serum albumin and hemoglobin suggests that the absorption mechanisms may be similar.

# ULTRASONIC ABSORPTION IN AQUEOUS SUSPENSIONS OF SMALL ELASTIC PARTICLES

Stephen Arthur Hawley, Ph.D.
Department of Biophysics
University of Illinois, 1967

The absorption of ultrasound has been measured in aqueous solutions of dextran, a quasi-linear anhydroglucose polymer, and in aqueous suspensions of small polystyrene particles over the frequency range 3 - 165 MHz. The absorption in dextran solutions has been found to be independent of molecular weight ( $10^4 \leq \overline{M}_w \leq 3.7 \times 10^5$ ) and substantially greater than would be anticipated from the dynamic shear viscosity contributions predicted on the basis of the Rouse theory. The absorption in aqueous polystyrene lattices has been measured in five suspensions with particle sizes ranging from 0.044 micron to 3.5 microns. Comparison of the absorption behavior to the Lamb-Urick-Epstein theory and to results obtained in bulk polystyrene reveal that neither relative motion nor internal viscosity of the particle contribute substantially to the observed acoustic attenuation. An Arrhenius dependence of absorption coefficient on temperature is observed in the lattices that indicates that dissipation of ultrasound is intimately associated with the liquid phase of the suspension. Comparison of the absorption properties of the lattices to that observed to that found in solutions of bovine serum albumin and hemoglobin suggests that the absorption mechanisms may be similar.

# ULTRASONIC ABSORPTION IN AQUEOUS SUSPENSIONS OF SMALL ELASTIC PARTICLES

Stephen Arthur Hawley, Ph.D.
Department of Biophysics
University of Illinois, 1967

The absorption of ultrasound has been measured in aqueous solutions of dextran, a quasi-linear anhydroglucose polymer, and in aqueous suspensions of small polystyrene particles over the frequency range 3 - 165 MHz. The absorption in dextran solutions has been found to be independent of molecular weight ( $10^4 \leq \overline{M}_w \leq 3.7 \times 10^5$ ) and substantially greater than would be anticipated from the dynamic shear viscosity contributions predicted on the basis of the Rouse theory. The absorption in aqueous polystyrene lattices has been measured in five suspensions with particle sizes ranging from 0.044 micron to 3.5 microns. Comparison of the absorption behavior to the Lamb-Urick-Epstein theory and to results obtained in bulk polystyrene reveal that neither relative motion nor internal viscosity of the particle contribute substantially to the observed acoustic attenuation. An Arrhenius dependence of absorption coefficient on temperature is observed in the lattices that indicates that dissipation of ultrasound is intimately associated with the liquid phase of the suspension. Comparison of the absorption properties of the lattices to that observed to that found in solutions of bovine serum albumin and hemoglobin suggests that the absorption mechanisms may be similar.

## ACKNOWLEDGMENT

The author is indebted to Professor Floyd Dunn for his continued interest and suggestions throughout the course of this investigation.

Support of this research by the Office of Naval Research, Acoustics Programs (Contract No. 1834 (29)) and by the National Institutes of Health, Institute of General Medical Sciences (Grant No. GM 12281) is gratefully acknowledged.

# ULTRASONIC ABSORPTION IN AQUEOUS SUSPENSIONS OF SMALL ELASTIC PARTICLES

BY

STEPHEN ARTHUR HAWLEY
A.B., Knox College, 1961
M.S., University of Illinois, 1963

THESIS

Submitted in partial fulfillment of the requirements
for the degree of Doctor of Philosophy in Biophysics
in the Graduate College of the
University of Illinois, 1967

Urbana, Illinois

# TABLE OF CONTENTS

# CHAPTER I

## INTRODUCTION

The absorption coefficient, $\alpha$ , of an acoustic plane progressive wave is defined by the relation

$$I_x = I_o e^{-2\alpha x}$$

where $I_x$ and $I_o$ are the coordinate-dependent and reference intensities, respectively. Although ultrasound is defined in the entire frequency range beyond the upper limit of human auditory perception at about 20 KHz (Hz = cycle/sec), the range in which the absorption coefficient may be efficaciously determined experimentally is somewhat less. In liquids, for example, $\alpha$ has been determined most successfully using a plane wave field configuration in the frequency range between about 100 KHz and 200 MHz. Because of the interest in the absorption coefficient, it is the latter frequency range that will be of primary concern in the ensuing discussions.

The use of ultrasonic propagation parameters, in particular the speed of sound and absorption coefficient, as a means of examining the molecular properties of matter represents a field of extensive experimental development over the last thirty years. Although the theoretical understanding of the problems has grown at a corresponding rate, much of the important ground work is attributed to workers of the classical era of physics, most notably, Stokes,

Kirchoff, and Rayleigh.

The recognition that acoustic parameters may be utilized to delineate the kinetics of rapid reactions near equilibrium is attributed to Einstein (1920). The principle of this method resides in the fact that the acoustic wave is an adiabatic and compressional phenomenon and its passage through a fluid results in rapid, periodic fluctuations of temperature and pressure which under appropriate circumstances may perturb a chemical reaction from equilibrium. The resulting relaxational interaction with the acoustic beam has a characteristic absorption behavior which will be described in more detail in Chapter II.

The investigation of the absorption properties of solutions of macromolecules is relatively recent and represents a point of convergence of at least two independent lines of research. One of these has arisen in conjunction with efforts to elucidate the mechanisms of absorption and interaction of high-intensity noncavitating ultrasound in biological materials. Another research interest has utilized ultrasonic absorption in solutions of polyamino acids in order to characterize helix-coil transitions which arise in the cooperative dissociation of hydrogen-bonding.

Although a number of investigations have been directed toward the characterization of ultrasonic absorption properties of solutions of macromolecules and a substantial amount of data accumulated, elucidation of the absorption mechanisms has been elusive. This is

primarily due to the disparity between the limited information contained in the acoustic data and the apparent complexity of the hydrodynamic properties of macromolecules. Edmonds (1966b) has suggested that the absorption in protein solutions may be due to the manifestation of as many as twenty-two molecular processes. This may be contrasted to the fact that in most macromolecular solutions studied thus far, the dependence of the absorption on frequency may be described in a simple polynomial form. Another problem may be traced to the fact that many of the processes responsible for absorption, e.g., dynamic volume viscosity, are unique to ultrasonic propagation. Thus, it is not usually possible to refer to other methods to provide parameters to delineate individual mechanisms.

The acoustic absorption properties of aqueous suspensions of the following macromolecules have been observed over a sufficient frequency range for comparison: hemoglobin (Carstensen et al., 1953, 1959b; Edmonds, 1962; Dunn et al., 1966), serum albumin (Carstensen et al., 1953), fractionated dextran (Hawley et al., 1965; Kessler, 1966) helical polyglutamic acid (Burke et al., 1965), and polyethylene glycol (Hammes and Lewis, 1966). Although a variety of tertiary structures are represented by these materials, the absorption properties exhibit the following characteristic similarities. 1) The absorption coefficient is proportional to concentration. This seems to be valid to concentrations of about 15%. Because the displacement of particles relative to the solvent due to the acoustic wave is of the order of a

few Angstrom units, it is not expected that the requirement of diluteness, to avoid intermolecular interactions, will be as stringent as in static flow experiments. 2) Extrapolation to zero concentration reveals that the absorption contributions of the polymer and the solvent are additive. 3) The excess absorption due to presence of the macromolecule is significantly greater than that observed in equivalent concentrations of monomer. Since only the soluble amino acids have been examined, there may be some uncertainty with regard to the natural proteins; however, it seems likely that the excess absorption is related to polymerization. 4) The excess frequency-free absorption $\alpha/f^2$ decreases with frequency and approaches the value of the solvent or slightly above it. Unfortunately this occurs in the region of the upper limit of frequency available by efficacious techniques so that high frequency behavior has not been determined precisely. 5) The frequency-free excess absorption for a significant portion of the available spectrum appears to be nearly proportional (excepting polyethylene glycol) to frequency raised to a small negative power. The apparent experimental error indicated for polyethylene observations does not, however, preclude it from this description.

Although an empirical description reveals a simple relation between absorption and frequency, it does not follow that the underlying mechanisms are also simple. For example, the absorption behavior has been attributed to a distribution of relaxation events whose corresponding

characteristic frequencies are distrubuted over the spectrum of interest. Assuming a continuous distribution Carstensen et al., (1959b), Edmonds (1962), and (Burke et al., 1965) have been able to fit empirically their data to curves generated by suitable distribution functions. The analyses are complicated by the disparity that exists between the low information content of the acoustic data and the highly specific requirements of meaningful analysis. Since a priori information concerning the molecular origin of the distribution function is not used in these cases, the meaning of such analyses is doubtful (as is recognized by the authors).

This investigation considers the absorption by aqueous suspensions of a flexible, linear polymer and an impermeable spherical, elastic colloid. The selection of these materials was predicated on the assumption that their absorption character would yield information about specific mechanisms that may be important in the absorption character of all polymer solutions. The macromolecules investigated to date have been almost exclusively polyelectrolytes whose absorption character may well be determined by such factors as the hydrophobic bonding, rigid tertiary structure, or electroviscous interactions (Dunn et al., 1966). It was felt that by employing a linear nonelectrolytic polymer, contributions to absorption from such effects could be eliminated and a more definable system provided.

Dextran, a linear (1-6) anhydroglucose polysaccharide was chosen because of its chemical stability, inertness,

and availability in the relatively large quantities of fractionated material required for ultrasonic characterization, viz., approximately 100g in the frequency range of interest. The molecular species is essentially a linear structure with 5 - 10% of the glucose residues existing as branching elements. In aqueous solutions it behaves essentially as that of a random coil with a small additional molecular dilation attributable to excluded volume effects associated with the branching structures (Granath, 1958). The ultrasonic absorption was measured in solutions of several fractions corresponding to weight-average molecular weights ranging from $10^4$ to $3.7 \times 10^5$.

The passage of an acoustic wave through a suspension of particles which have a density different from that of the surrounding medium will produce relative motion between the particles and the fluid. The dissipation of acoustic energy that results from Stokes frictional losses has been described theoretically by Lamb, 1945; Epstein, 1941; Urick, 1948; Angerer et al., 1951; and Fry, 1952. For particles in the size range of macromolecules, this theory predicts a negligible contribution to the total absorption behavior. It has been found, however, that the propagation of high-intensity noncavitating ultrasound through solutions of DNA will produce molecular degradation (Frontali, 1962; Hawley et al., 1963). Both the mechanical stresses that appear in the liquid and the force gradient that is attributable to relative motion are too small to account for the degradation

(Macleod, 1966). In order to verify the magnitude of the viscous losses at small particle diameters, absorption measurements were conducted in dispersions of polystyrene spheres.

The absorption in five aqueous polystyrene lattices with particle radii ranging from .044 micron to 3.5 micron has been measured. Four of the suspensions are of the monodisperse species utilized as secondary standards in electron microscopy.

# CHAPTER II

## THEORY

### A. Relaxation Phenomena

It seems appropriate to interpret first the acoustic implications of mechanical relaxation, a concept which is found to pervade virtually all mechanisms associated with acoustic attenuation. When a steady state stress applied to a real liquid is instantaneously released, it is found that a finite time is required for the disappearance of the associated strain. The time delay may arise from any of a number of mechanisms and is a reflection of the molecular properties of the liquid (Herzfeld and Litovitz, 1958). If the stress is associated with excess pressure and strain with excess density, the time dependence of the excess density, $\delta\rho$, may be written as

$$\delta\rho = \delta\rho_0 e^{-t/\tau}$$

where $\delta\rho_0$ is the steady state excess density and $\tau$ is the relaxation time.

When the stress is periodic, as is the case with the propagation of ultrasonic energy, the relaxation events are manifested as a frequency-dependent phase lag between pressure and density. The persistence of the phase difference requires work to be performed on the liquid at the expense of acoustic energy. The result is a frequency-dependent absorption coefficient, viz.,

$$\frac{\alpha}{\omega} = \frac{K\omega/\omega_r}{1+(\omega/\omega_r)^2} \qquad (2\text{-}1)$$

where $\omega_r = 1/\tau$

and $\omega$ is the angular frequency $2\pi f$, K is a constant and $\omega_r$ is the relaxation frequency (Kinsler and Frey, 1962). When $\omega_r >> \omega$, it is evident that the excess density will closely follow the pressure variations with a small phase lag. When $\omega_r << \omega$, the relaxation process is not perturbed and again the associated phase retardation will be small. The variation of the quantity $\alpha/\omega$ as a function of frequency exhibits a peak when $\omega\tau = 1$, and K may be evaluated in terms of the maximum value, $(\alpha/\omega)^*$. Summarizing these ideas: when $\omega = \omega_r$

$$\frac{\alpha}{\omega} = \frac{K}{2}\left(\frac{\alpha}{\omega}\right)^*$$

thus

$$\frac{\alpha}{\omega} = 2\left(\frac{\alpha}{\omega}\right)^* \frac{\omega/\omega_r}{1+(\omega/\omega_r)^2}$$

so that when $\omega << \omega_r$

$$\frac{\alpha}{\omega^2} = \frac{2}{\omega_r}\left(\frac{\alpha}{\omega}\right)^* = \text{CONSTANT}$$

and when $\omega >> \omega_r$

$$\alpha\omega = 2\omega_r\left(\frac{\alpha}{\omega}\right)^* = \text{CONSTANT}$$

Examination of (2-1) reveals that a fairly broad peak is determined by a single relaxation event. Generally about a

two decade frequency span is required to delineate accurately the relaxation event (Davies and Lamb, 1957).

The possible origins of relaxation events in terms of molecular mechanisms are multifold. For example, compressional energy may be coupled to internal degrees of freedom associated with specific heat (thermal relaxation) or it may perturb configurational transitions between states of different specific volumes (structural relaxation), (Herzfeld and Litovitz, 1959). Coupling of acoustic energy to a molecular transition is an equilibrium process described kinetically for the transition between two states by the usual rate equation:

$$[A] \underset{K_2}{\overset{K_1}{\rightleftharpoons}} [B]$$

The equilibrium is most effectively perturbed at frequencies determined by the rate constant. For the above reaction the relaxation frequency is

$$\omega_r = 1/\tau = \frac{1}{K_1 + K_2}$$

When a single relaxation event prevails, ultrasonic methods may be gainfully employed in the analysis of molecular transitions with time constants between about $10^{-5}$ and $10^{-10}$ seconds (Hammes, 1966). For a two state equilibrium isothermal reaction, the expression for the molar free energy change $\Delta G$ is

$$\Delta G = \Delta H - T\Delta S = \Delta U + P\Delta V - T\Delta S$$

where $\Delta H$, $\Delta U$, $\Delta V$, $\Delta S$, and $P$ are the molar changes in

enthalpy, internal energy, volume, entropy and pressure, respectively. Determination of $\Delta G$ from acoustic parameters is possible when either of two assumptions is valid: 1) when $\Delta V \neq 0$, $\Delta U = 0$ and 2) when $\Delta U \neq 0$, $\Delta V = 0$ (Dunn, et al., 1966). The processes described by conditions 1) and 2) are usually referred to as structural and thermal relaxations, respectively.

The most useful feature of the absorption spectrum in delineating relaxation processes is the peak in that occurs when $\omega\tau = 1$. If a simple two-state reaction prevails in which the rate is determined by an activation energy barrier $\Delta G^{\ddagger}$, it can be shown that the relaxation time is of the form (Litovitz, 1959)

$$\tau = Ke^{\Delta G^{\ddagger}/RT}$$

where K is a constant. Thus, by determining the temperature dependence of $\tau$, it is possible to evaluate the associated activation energy.

When more than one relaxation time is involved, the situation becomes more complicated and the quantity $(\alpha/\omega)$ is given by

$$\frac{\alpha}{\omega} = 2\sum_{n=1}^{N}\left(\frac{\alpha}{\omega}\right)_n^* \frac{\omega/\omega_n}{1+(\omega/\omega_n)^2} \qquad (2\text{-}2)$$

for N noninteracting relaxation events. Because (2-2) represents the summation of slowly varying functions, it can be seen that the individual relaxation behaviors mask each other at a relatively low density of relaxation events per frequency interval. When the absorption can be traced to processes

which are governed by a continuum of relaxation times, (2-2) takes the integral form (Carstensen and Schwan, 1959b)

$$\frac{\alpha}{\omega} = \int_{\omega_{r_1}}^{\omega_{r_2}} \frac{f(\omega_r)\,\omega/\omega_r}{1 + (\omega^2/\omega_r^2)}\, d(\omega_r) \qquad (2\text{-}3)$$

B. Viscosity

At least a portion of the total absorption in all real liquids is due to the finite viscosity of the fluid and since viscous interactions impose a limit on the rate of molecular flow, it may be considered a relaxation process. Passage of a longitudinal acoustic wave through a liquid is accompanied by both shear and volume deformations of the lattice. Energy dissipation that occurs in the production of molecular translation is related to shear viscosity. Volume viscosity is generally associated with the creation and extinction of vacancies in the liquid with a relaxation time related to the rearrangement of molecules surrounding a vacancy (Herzfeld and Litovitz, 1955). In addition, if the liquid exhibits elastic response to mechanical stresses, the viscosities include an imaginary component. Thus,

$$\eta_v^* = \eta_v' - i\eta_v''$$
$$\eta_s^* = \eta_s' - i\eta_s'' \qquad (2\text{-}4)$$

where the subscripts v and s refer to volume and shear deformational modes, respectively. The viscosities can be related to the corresponding bulk and shear moduli, i.e., the complex stress-strain ratios by

$$K^* = i\omega\eta_v^*$$
$$G^* = i\omega\eta_s^* \qquad (2\text{-}5)$$

so that $\eta_v' = K''/\omega \; ; \; \eta_v'' = K'/\omega$

$$\eta_s' = G''/\omega \; ; \; \eta_s'' = G'/\omega \qquad (2\text{-}6)$$

The quantities G' and K' are usually referred to as the storage moduli as they are a measure of the stored dynamic energy. G" and K" are a measure of the heat loss per cycle and are correspondingly referred to as the loss moduli (Ferry, 1961). The dependence of the acoustic properties on the viscoelastic parameters are revealed by examination of the solution of the wave equation that can be derived from the Stokes-Navier hydrodynamic equations generalized to include a volume viscosity. The wave equation that arises is

$$\frac{\partial^2\xi}{\partial t^2} = \frac{[K^* + (4/3)\,G^*]}{\rho}\,\frac{\partial^2\xi}{\partial x^2}$$

where is density and is the displacement of a point in the medium. Using the procedure of Litovitz and Davis (1964), the velocity of a periodic disturbance is given by

$$V = \frac{[K^* + (4/3)\,G^*]^{1/2}}{\rho^{1/2}}$$

Assuming the presence of an absorption coefficient such that

$$\xi = \xi_0 e^{\{i\omega\tau - (\alpha - i\omega/V)x\}}$$

then

$$R_e\left\{K^* + (4/3)G^*\right\} = \rho V^2 \left\{\frac{1 - \left(\frac{\alpha V}{\omega}\right)^2}{\left[1 + \left(\frac{\alpha V}{\omega}\right)^2\right]^2}\right\}$$

$$I_m\left\{K^* + (4/3)G^*\right\} = \frac{2\rho V^2\left(\frac{\alpha V}{\omega}\right)}{\left[1 + \left(\frac{\alpha V}{\omega}\right)^2\right]^2} \qquad (2\text{-}7)$$

The quantity $\left(\frac{\alpha V}{\omega}\right)$ will be sufficiently small, viz., $< 10^{-2}$ for the materials of interest and equations (2-7) reduce to

$$K' + (4/3)G' = \rho V^2 \qquad (2\text{-}8)$$

$$K'' + (4/3)G'' = \frac{2\rho V^3 \alpha}{\omega} \qquad (2\text{-}9)$$

By combining (2-8) and (2-9) we have the relation

$$\frac{\alpha}{\omega} = \frac{\rho^{1/2}\left(K'' + (4/3)G''\right)}{2\left[K' + (4/3)G'\right]^{3/2}} \qquad (2\text{-}10)$$

Utilizing the relations between viscosities and moduli, (2-9) becomes

$$\frac{\alpha}{\omega^2} = \frac{1}{2\rho V^3}\left[\eta_v' + (4/3)\eta_s'\right.$$

At sufficiently low frequencies $\eta_s'$ and $\eta_v'$ may be represented by their static flow values and the result is essentially the same as that derived by Stokes in 1945, viz., in the ab-

sence of experimental evidence, he assumed that

$$\eta_v' \approx 0$$

so that

$$\alpha = \frac{\omega^2}{2\rho V^3} \eta_s' \qquad (2\text{-}11)$$

In liquids, (2-11) constitutes what is usually referred to as the classical absorption coefficient. In general, the bulk viscosity does not vanish so that (2-11) often predicts values lower than are obtained experimentally.

The relaxation time associated with shear viscosity is given by (Kinsler and Frey, 1962)

$$\tau = (4/3) V^3 \rho \eta_s'$$

For water at 20.0°C, this corresponds to a relaxation frequency greater than $10^{12}$ Hz, which is out of range of the conventional experimental technology. If the excess absorption over the classical value is associated with bulk viscosity, the corresponding relaxation time is of the same order of magnitude as that due to shear processes.

## C. Dynamic Viscosities Of Solutions Of Random Coil Polymers

Generally the static flow viscosity does not describe adequately the dynamic properties of macromolecular suspensions. Equations (2-4) and (2-5) provide a more general form. Examination of these equations reveals, however, that determination of $\alpha$ and V for longitudinal wave propagation does not permit the separation of the contributions due to the bulk and shear moduli. Thus, without independent

information, assumptions concerning the relative behavior of moduli are necessary.

Theoretical treatment of the dynamic shear viscoelastic properties of dilute solutions of flexible polymers lead to a distribution function (Rouse, 1953) that shows good agreement with experimental evidence (Rouse and Sittel, 1953). The arguments evolve from a molecular model (Zimm, 1963) represented by a chain of massless beads connected by Hookean springs which is suspended in a viscous liquid. Free rotation of the segments is permitted about each bead and the molecule is assumed to be long enough to permit a Gaussian distribution of end-to-end chain lengths. Neglecting hydrodynamic interaction of segments, a "free draining" model is established (Rouse, 1953); the more general treatment (Zimm, 1956) accounts for this interaction and is referred to as the "non-free-draining" case. For the Rouse theory, the prediction for the dynamic moduli are

$$G' = nkT\sum_{p=1}^{N} \frac{\omega^2 T_p^2}{1+\omega^2 T_p^2} \qquad (2\text{-}12)$$

$$G'' = \omega\eta_0 + nkT\sum_{p=1}^{N} \frac{\omega T_p}{1+\omega^2 T_p^2} \qquad (2\text{-}13)$$

where $\eta_0$ is the solvent viscosity, k is Boltzman's constant, T is absolute temperature, n is the number of polymer molecules per unit volume and N is the minimum number of submolecules such that random distribution of end-to-end distances is observed (see for example, p. 159, Tanford,

1961). The origin of the viscoelasticity is statistical. Deformation of the molecule by an external force requires energy since it results in a deviation from random behavior and thus a decrease in configurational entropy. Because a finite time is required for reestablishment of random orientation, some of the energy is stored in the transient non-Gaussian average orientation. In addition, the total configurational behavior is described by a large number of internal molecular modes and corresponding relaxation times ($\tau_p$). At low frequencies the viscosity is dominated by the primary mode ($p = 1$) which corresponds to the translation of the center of gravity (Rouse, 1953). The corresponding relaxation time is determined by

$$\tau_1 = \frac{6 M \eta_s [\eta]_o}{\pi^2 R T} \qquad (2\text{-}14)$$

where M is the molecular weight (Zimm, 1956). This mode contributes about 66% of the static viscosity. The individual importance to low frequency behavior of the other modes decreases as the portion of the total molecule concerned becomes shorter.

The contribution of the dynamic shear viscosity to the ultrasonic absorption of solutions of random coil polymer can be evaluated in terms of the Rouse theory. By combining (2-8) and (2-9) with (2-13) the following relation results:

$$\frac{\alpha}{\omega} = \frac{\left[ K'' + 4/3 \left( \omega \eta_o + nKT \sum_{p=1}^{N} \frac{\omega \tau_p}{1 + \omega^2 \tau_p^2} \right) \right]}{2 \rho V^3} \qquad (2\text{-}15)$$

Separating the shear from the volume viscous contributions

$$\frac{\alpha_s}{\omega} = \frac{2}{3}\,\frac{\left(\omega\eta_o + nKT\sum_{p=1}^{N}\frac{\omega\tau_p}{1+\omega^2\tau_p^2}\right)}{\rho V^3} \qquad (2\text{-}16)$$

where $\alpha_s$ is the absorption related to shear viscosity only. In the frequency range of interest in the present investigation (3-150 MHz), the period of the wave will be, generally, somewhat shorter than the primary relaxation time. In this regard (2-13) may be written as (Rouse, 1953)

$$G'' = \omega\eta_o + \frac{3\omega(\eta_s-\eta_o)}{\pi(2\omega\tau_1)^{1/2}} \qquad (2\text{-}17)$$

provided that $2 < \omega\tau_1 < N^2/250$

where $\eta_s$ is the steady state shear viscosity. For sufficiently dilute solutions (Zimm, 1956)

$$\frac{\eta_s-\eta_o}{\eta_o c} = [\eta]_o \qquad (2\text{-}18)$$

where $[\eta]_o$ is the intrinsic viscosity. Thus, by incorporating (2-17) and (2-18) into (2-16) the shear absorption is obtained in terms of steady state molecular parameters

$$\frac{\alpha_s}{\omega^2} = \frac{\rho_o V_o^3}{\rho V^3}\left[\frac{\alpha_{o,s}}{\omega^2} + \frac{3\eta_s[\eta]_o c}{\pi(\rho_o V_o^3)(2\tau_1\omega)^{1/2}}\right] \qquad (2\text{-}19)$$

$$2 < \omega\tau_1 < N^2/250$$

where $\rho_o$, $V_o$ and $\alpha_{o,s}$ are the density, velocity and Stokes absorption in the solvent, respectively. In dilute solutions $\frac{\rho_o V_o^3}{\rho V^3} \approx 1$, since the macroscopic com-

pressibility of a liquid will not be appreciably affected by the presence of a small concentration polymer molecules (Mason, 1961). Thus for dilute solutions we may write

$$\frac{\alpha_s}{\omega^2} = \frac{\alpha_{o,s}}{\omega^2} + \frac{3\eta_s[\eta]_o c}{\pi(2\omega\tau_1)^{1/2}\rho_o V_o^3} \qquad (2\text{-}20)$$

Unfortunately, a derivation of a quantitative relation between the volume viscosity and molecular parameters is not as clearly provided as it is in the case of shear viscosity. For solutions of random coil polymers, however, it is possible to make a few observations on the nature of such a viscosity component. Any change in the apparent volume viscosity of a liquid that may result from the addition of a random coil polymer must arise from an interaction with the solvent. This is based on the premise that the volume viscosity is related to the structural mobility of clusters of neighboring molecules, a situation which is clearly not provided by the polymer segments considered by themselves. If the affinity of polymer segments for the solvent is identical to the affinity between solvent molecules, the presence of polymer would not be expected to generate regions of high structural viscosity. Thus, a significant volume viscosity can be developed only by the formation of a polymer-solvent complex. The nature and extent of the complex are determined in part by the interaction between monomer and the solvent as well as by any cooperative effects that become manifest in polymerization,

e.g., arising from periodicity or immobilization of the monomer unit.

## D. Lamb-Epstein-Urick Theory Of Acoustic Attenuation In Suspensions of Small Particles: Relative Motion

The absorption of sound by a suspension of small spherical objects is treated generally by Epstein (1941). By solving the Stokes-Navier hydrodynamic equations one can obtain the following expression for suspensions of particles that are small compared to a wavelength. It is additionally assumed that the shear rigidity of the particle is large with respect to the suspending fluid.

$$\alpha = \frac{c_v\left(\rho_0/\rho_p - 1\right)R}{2(V/\omega)}\left\{\frac{i + b - ib^2/3}{\left(\frac{\rho_0}{\rho_p}\right) - i\left(\frac{\rho_0}{\rho_p}\right)b - \left(2+\frac{\rho_0}{\rho_p}\right)b^2/9}\right\}$$

where

$$b^2 = \frac{i\omega\rho_0 R^2}{\eta_0}$$

and R is the particle radius, $\rho_p$ is the particle density, $c_v$ is the volume fraction of the particles, $\rho_0$ , $\eta_0$ are the density and viscosity of the suspending liquid, respectively. The real part of this expression may be extracted by using the parameter (Carstensen and Schwan, 1959a)

$$\gamma^2 = \rho_0 R^2/2\eta_0$$

so that

$$b^2 = 2i\gamma^2\omega$$

The expression for the absorption becomes

$$\alpha = \frac{2}{9}\frac{C_v}{V}\left(1-\frac{\rho_o}{\rho_p}\right)^2\left\{\frac{\gamma^2\omega^2\left[1+\gamma\omega^{1/2}\right]}{\left[1+\gamma\omega^{1/2}\right]^2+\gamma^2\omega\left[1+\frac{2}{9}\left(\frac{2\rho_o}{\rho_p}+1\right)\gamma\omega^{1/2}\right]^2}\right\} \quad (2\text{-}21)$$

Epstein interprets the origin of this absorption as the result of conversion of longitudinal wave energy to shear waves at the interfaces between particle and the suspending fluid. Since shear waves are highly damped in fluids, energy converted to this form is degraded as heat. As the diameter of the particle is increased with respect to the wavelength, two addition terms are necessary: first, as a correction for (2-21) and second, as a scattering term. The first of these takes the form

$$\Delta\alpha = \frac{C_v\omega^3R^2}{V^3}\,R_e\left\{(10/9b)+(23i/4b^2)\right\}$$

when

$$\frac{\rho_p}{\rho_o} \approx 1$$

Reducing this as above,

$$\Delta\alpha = \frac{C_v\omega^3R^2}{V^3\gamma\omega^{1/2}}\left[\frac{5}{9}+\frac{23}{8\gamma\omega^{1/2}}\right] \quad (2\text{-}22)$$

This scattering term is

$$\alpha_s = \frac{C_v\omega^4R^5}{V^4}\left[\frac{\left(\frac{\rho_p}{\rho_o}-1\right)^2}{\left(\frac{\rho_p}{\rho_o}+2\right)^2}+\frac{1}{3}\left(1-\frac{K_o'}{K_p'}\right)^2\right] \quad (2\text{-}23)$$

where $K_p'$ and $K_o'$ are the real parts bulk moduli of the

particle and liquid, respectively.

Although Epstein indicates that the losses due to relative motion of the liquid and the particle are included in (2-21), the extent of this contribution is not immediately obvious.

Urick (1947) developed an expression that relates the absorption coefficient to the relative motion losses. The identical result is obtained by extending the arguments of Lamb (1945) and also by considering the motion of a pendulum in a viscous liquid. In Urick's notation this is

$$\alpha' = \frac{2}{3}\pi R^3 \left(\frac{\rho_0}{\rho_p} - 1\right)^2 \left\{\frac{S}{S^2 + (\sigma + T)^2}\right\} \qquad (2\text{-}24)$$

where

$$T = 1/2 + 9/4\beta R$$

$$S = (9/4\beta R)(1 + 1/\beta R)$$

$$\beta = \left(\frac{\omega\rho}{\eta_0}\right)^{1/2}$$

This may be compared to the Epstein value by substituting

$$\beta = \frac{\gamma\omega^{1/2}}{R}$$

with the interesting result that expressions (2-21) and (2-24) are identical. Other approaches have led to an equivalent relation (Angerer, Barth and Guttner, 1951). Thus, as Carstensen and Schwan (1959a) point out, Epstein's concept of mode conversion is apparently a quantitative description of local shear flow of the suspending liquid relative to the particle surface.

The Lamb-Epstein-Urick theory has been found adequate

in describing the absorption in dispersions of rigid particles such as glass beads (Busby and Richardson, 1956) and san and Kaolin (Urick, 1948; Stakutis et al., 1955; Hueter, 1958). Studies conducted in suspensions of polymethyl methacrylate (Wada et al., 1960), however, reveal an absorption coefficient somewhat higher than predicted by (2-21) and (2-24). The disparity has been attributed by Wada et al., (1960) to the volume viscoelasticity of the particle with the contention that the difference between the observed absorption and that predicted by the Lamb-Epstein-Urick theory is given by

$$\alpha_E = \frac{K_o K_p'' C_V \omega}{2 V (K_p')}$$

where $\alpha_E$ is the absorption due to the volume viscosity of the particle whose complex bulk modulus is determined by $K_p'$ and $K_p''$ ; $V$ is the velocity of sound in the suspension. In arriving at this relation, the authors have assumed that the shear rigidity of the particle is sufficiently large that the shape deformation by the acoustic is negligible.

# CHAPTER III

## EXPERIMENTAL

### A. Pulse Technique

The effective exploitation of ultrasonic spectroscopy has developed over the last thirty years into a useful technique for the characterization of matter. Methodology employed for liquids is diverse, however, and falls roughly into two classes; continuous wave techniques and pulse techniques.

Early investigators (before 1945) employed continuous wave methods exclusively. The absorption of a coherent, plane longitudinal wave train in a liquid can be related to both its standing wave interferometric behavior and also to the ability of the wavefronts to act as an optical diffraction grating (Debye-Sears effect), (Klein et al., 1965). These techniques are not particularly effective over a wide frequency range or whenever the attenuation is large (Hueter and Bolt, 1960). Because the existence of an absorption coefficient requires the dissipation of acoustic energy as heat, temperature fluctuations become a serious problem when the absorption becomes large. This is particularly true of interferometric techniques in which virtually all the acoustic energy is absorbed in the sample (Pinkerton, 1949). There are other problems with continuous wave techniques (Hueter and Bolt, 1960) which restrict their usefulness in liquids and as such will

not be dealt with further here.

Pulse techniques were introduced to ultrasonic absorption and velocity measurements in liquids by Pellam and Galt (1946), Pinkerton (1947, 1949), and others as a natural outgrowth of the radar technology developed during World War II. At the basis of this method is the determination of the relative pressure amplitude of a short burst of ultrasonic energy after it has been allowed to propagate for specified distances in a test medium. The generation and detection of pulses can be accomplished in either of two ways; by a transmission method requiring two transducers such that one acts as the source and the other as receiver; or by a reflection method requiring a single transducer and a reflecting surface so that the transducer becomes both source and detector. The immediate advantage of this technique over continuous wave methods is that while the peak intensity of the pulse may be maintained at a high level, the average intensity of the signal propagated in the medium is kept sufficiently small by using a low duty cycle ($10^{-3}$) so that temperature stability problems are avoided. Further, the short acoustic transients that are characteristic of pulsed methods preclude problems that may develop in connection with the appearance of undesirable standing waves. Increased frequency range and less stringent restrictions on the absorption property of the sample are the net result.

There are a number of adaptations of the pulse technique available which permit the exploration of the

frequency range from 300 KHz to 500 MHz (Carstensen, 1954; Edmonds et al., 1962; Andreae and Joyce, 1962; Hunter and Dardy, 1965). A single experimental configuration, however, is limited to somewhat less than two decades of frequency. The frequency limitations imposed on this method are essential in absorption cell design consideration and are discussed below. For the purposes of acoustic spectroscopy, ultrasonic energy can be both generated and detected by proper accomodation of the piezoelectric phenomenon. Longitudinal waves are conveniently produced from a wafer of quartz, cut perpendicular to the crystalline x-axis and with metal electrodes deposited on the major faces (Mason, 1950). Effective transduction of electrical energy applied to the electrodes to mechanical vibrations occurs at frequencies such that the thickness of the wafer corresponds to an odd number of half wavelengths. Inversely, an oscillatory mechanical stress of the appropriate frequency results in the development of an electrical potential of the same periodicity. The relation between fundamental resonant frequency and thickness for generation of longitudinal waves in liquids is given (for quartz) by

$$f = \frac{c}{2t} \quad \frac{2.875 \times 10^5}{t} \quad \text{sec}^{-1},$$

where f is frequency, c is speed of sound in quartz ($5.75 \times 10^5$ cm/sec) and t is the thickness in cm. Transducers may also be operated at the odd harmonies of the fundamental frequency. Thus, frequency cannot be

used effectively as a continuous variable and is limited to discrete values. This is not a serious handicap, however, since acoustic variables in general do not exhibit rapid fluctuation with frequency (Litovitz, 1959).

## B. Experimental Design Considerations

### 1. Diffraction

The diffraction pattern of a plane transducer acting as a piston source is similar to that of a beam of light passing through a circular aperture (Kinsler and Frey, 1962). The field for a source radiating into a semi-infinite medium is composed of a near Fresnel region and the far or Fraunhofer field. Demarcation between these two regions is usually set at the zero order maximum of the near field at a distance z from the source such that $z \simeq R^2/2\lambda$ (Hueter and Bolt, 1960) (where R is the radius of the source and $\lambda$ is the wavelength in the medium). The important features of the Fresnel region for the purposes of pulse measurements are that for a source large with respect to the wavelength only a small amount of beam divergence occurs in the Fresnel region and the criteria for plane waves are satisfied. In the Fraunhofer region the beam intensity becomes more diffuse as the main portion of the beam spreads at an angle $\Theta$ determined by $\sin\Theta = 0.61\lambda/R$. In an infinite medium, the wavefronts become spherical at large distances from the source with the intensity decreasing as $\frac{1}{Z^2}$.

Since the receiving transducers are of finite dimensions, the experimental design is such that measurements

are usually confined to the Fresnel region where the entire beam may be intercepted by the detector. In practice this restricts the maximum acoustic path length to less than $R^2/2\lambda$ (Pinkerton, 1949). The requirement that the radius of the source be large with respect to wavelength is satisfied by making its diameter at least 50 wavelengths (Nozdrev, 1965). For a cylinderical geometry with the direction of propagation along the axis, the requirement of an infinite baffle (semi-infinite medium) is satisfied by making the radius of the container at least twice that of the source transducer (Del Grosso, 1965). If this condition is not met, analyses become complicated by guided wave propagation resulting from reflections off the walls of the container. If a single path system is used, the receiving transducer should be at least as large as the source so that beam spread losses are kept at a minimum (Andreae et al., 1958). If the above conditions are met, the resulting diffraction will be of a free field form (Del Grosso, 1964). At low frequencies, however, the diffraction losses may still be large relative to the intrinsic absorption in the liquid. This is particularly true of water, aqueous solutions, and other materials with a small absorption coefficient below about 5 MHz (Del Grosso, 1964). The rather complete characterization free field diffraction by Del Grosso (1964, 1965) has made it possible to define adequately the system under these conditions and apply suitable corrections, thereby allowing the useful frequency

range of the apparatus to be extended below that where diffraction losses are negligible.

Satisfaction of the above requirements for free field diffraction place a nominal lower limit on the frequency range at which meaningful measurement of absorption can be made. For water and other low absorbing materials, this limit is about 500 KHz (see Appendix II). In addition, and more important for the study of some biological materials is that a minimum sample volume is required. It is found (Appendix II) that at 1 MHz about 5-10 liters of sample are needed to determine the absorption coefficient in water with the volume required decreasing with the square of frequency.

The volume requirement is a particularly stringent one in the consideration of some biological materials. This is especially true of purified proteins and highly fractionated macromolecular preparations. An additional difficulty is that the absorption coefficient for aqueous suspensions is usually rather low so that concentrations of 3 - 10% are generally required for characterization. Thus the investigation of purified enzyme preparations over a wide frequency range is prohibited by the expense required for materials. There are a few materials like bovine serum albumin and hemoglobin which are somewhat more readily available. It was thus decided that a maximum volume of about one liter of appropriate concentration could be tolerated, corresponding to a lower frequency limit of about 3 MHz. The low frequency characteristics of the

chamber were thereby fixed and are tabulated in Table 3-1.

TABLE 3-1

LOW FREQUENCY CHARACTERISTICS OF CELL AT 3MHz WITH WATER (20°C) AS TEST MATERIAL.

| | |
|---|---|
| $\lambda$ | 0.05cm |
| $R/\lambda$ | 25.4 |
| $R^2/\lambda$ | 32.2cm |
| $R'/R$ | 3.5 |

MAXIMUM TRANSDUCER SEPARATION 21.3cm

2. High Frequency Limitations

As frequency is increased, the problems associated with diffraction are alleviated. This follows from the fact that as the limit ($R^2/\lambda$) of the Fresnel field extends further into the medium, measurements are made over a smaller fraction of the diffraction pattern where the associated losses become negligible. Diffraction corrections are usually unnecessary above 15 MHz (Carome and Witting, 1960).

There are, however, a definite set of problems associated with high frequency measurements. The maximum acoustic pulse amplitude available is limited by the dielectric strength of the transducer material and mounting. For the quartz, the maximum voltage gradient that can be applied is about 1.5 kv/mm (Nozdrev, 1965). In a Stokes liquid the absorption coefficient increases with the square of

frequency so that with a limitation of pulse amplitude measurements at higher frequencies must be made at correspondingly shorter path lengths. With the transducers exposed directly into the medium, it is found that when the transit time of the pulse in the medium is less than about 10 microseconds, difficulty is encountered due to the time proximity of the rf driving pulse and the received signal. This is particularly true when the single transducer system is used since the oscillator and receiver are not electrically isolated. Even with the double transducer system it is extremely difficult to prevent some rf pickup by the high gain receiver. Thus, in order to produce a suitable time separation of the driving pulse and the received signal, the procedure of introducing an acoustic delay line is usually employed. This is accomplished by attaching the transducers to a rod of low loss material of the same acoustic impedance in such a way as to increase the acoustic path length without introducing attenuation (Andreae, 1958). Generally, fused quartz or silica is used for this purpose. Application of this technique allows the path length in the sample to be decreased to virtually zero without introducing electronic difficulties.

The high frequency limit of the complete apparatus depends ultimately on the mechanical precision of the moving parts. 510 MHz has been achieved (Hunter and Dardy, 1965) by maintaining transducer parallelism to better than $2.5 \times 10^{-4}$ cm/cm (about one wavelength in their test medium) and by measuring distance increments of 0.25 microns.

For the purposes of this work, an upper frequency limit of about 170 MHz was decided to be satisfactory. This eases the mechanical precision requirements to the extent that satisfactory parts can be fabricated in the laboratory machine shop and also obviated the need for a separate high frequency chamber. It has been found that with extreme care the final apparatus is capable of satisfactory operation at 200 MHz.

3. Velocity

Because of the importance of the absorption coefficient, velocity was given secondary consideration in the design of the apparatus. For the materials of interest here, the magnitude of the velocity dispersion requires that velocity measurements be accurate to at least one part in $10^4$ (Carstensen and Schwan, 1953). Accuracies of better than one part in 30,000 have been achieved (Del Grosso, et al, 1954), but because it would require a sacrifice of versatility of absorption measuring capability, the apparatus was constructed with the usual pulse ranging method of velocity measurement in mind (i.e., an accuracy of about 1%) (Pellam and Galt, 1946). Late in the investigations a somewhat new technique of velocity measurement was discovered which permits an accuracy of about 3.5 parts per 1,000. This method, in which the apparatus is used as an automatic recording interferometer, is found to be extremely useful in cross-checking other characteristics of the system such as distance measurements and temperature stability. Salient

aspects of this interferometric method will be discussed in detail below.

4. Temperature Control

The maintenance of accurate temperature control for absorption measurements is particularly crucial when aqueous materials are concerned. This may be attributed to the relatively large temperature dependence of the absorption coefficient that occurs for water (Figure 3-11). If the per cent deviation of the absorption coefficient per degree centigrade ($\frac{1}{\alpha}\frac{\partial \alpha}{\partial T}$ x 100) is computed, it is found that for water at 20°C there exists a 10% per degree dependence. Thus, to preclude an $\pm$ 1% error due to temperature uncertainty, knowledge and control of temperature to $\pm$ 0.1°C is required.

In addition, local fluctuations in temperature may result in refraction of the acoustic beam and lead to deterioration of instrument stability and accuracy (Edmonds, 1966a). Constant mixing of the liquid is generally recommended.

5. Semi-Automatic Recording Facility

The effective measurement of absorption usually involves point to point determination of pulse amplitude and acoustic path lengths (see for example, Pellam and Galt, 1946). The amplitude is measured at a large number of increments over an appropriate distance. Resulting points are usually plotted in a semi-logarithmic fashion so that where $p = p_o e^{-2\alpha x}$ a straight line results with the attenuation per unit path length as the slope. It was found in the preliminary

measurements associated with this study that this technique is both tedious and time consuming and thus prompted a consideration of a semi-automatic recording facility.

Andreae and Joyce (1962) describe an instrument which allows the direct display of the attenuation of the pulse amplitude as a function of distance. This is accomplished by inserting a servo-motor driven piston attenuator in such a manner that the amplitude of the pulse that is applied to the receiver is maintained at a constant level. The attenuator provides a constant attenuation insertion per unit distance and its movement is mechanically coupled to a recorder pen so that the deflection is a direct indication of pulse attenuation. The movement of the recorder paper is linked mechanically to the drive system which governs the acoustic path length so that an accurate correspondence is maintained. Because of the complexity of this apparatus its fabrication was not attempted. Using this system as a starting point, however, a somewhat simpler instrument was developed which differs from the above described apparatus in several respects.

## C. Design

### 1. Mechanical

The instrument is designed to be used in two configurations corresponding to two frequency ranges; a low and intermediate range (LI) from 3-87 MHz and a high frequency range (H) covering 75-165 MHz. Operation in both ranges was accomplished for the most part with the same mechanical components in slightly different orientation.

Appropriate transducer displacement was found to be most conveniently achieved by employing a piston-cylinder arrangement (Edmonds et al, 1962). A piston with a transducer centered on the face (Figure 3-4) is driven within a cylindrical chamber that contains an identical transducer mounted in the base. By using the walls of the cylinder as a guiding surface, it was found that stable and uniform motion can be obtained.

All machined parts which come in contact with the sample are fabricated from stainless steel 316. The chamber (Figure 3-1) is a precision ground cylinder with a bore of 3.5 inches and effective length of 9 inches. The piston assembly is driven vertically within the cylinder. The piston rod is a one inch stainless tube which is precision ground ($\pm$ 0.0002 in.) along its entire length. Both ends of the rod are internally threaded so as to accomodate a transducer assembly at one end and an actuator screw at the other. The rod has a half inch internal diameter to allow the passage of RG-62-U cable and associated rf connectors to effect a stable electrical connection to the transducer. A small transverse hole near the top provides the necessary cable exit.

The piston head is a cylinderical block of stainless steel having a length of two and one half inches. Because stainless steel provides a notably poor bearing surface, Teflon O-rings are employed in order that a small clearance with the cylinder wall could be tolerated without fear of mechanical seizure. A one inch diameter hole bored along

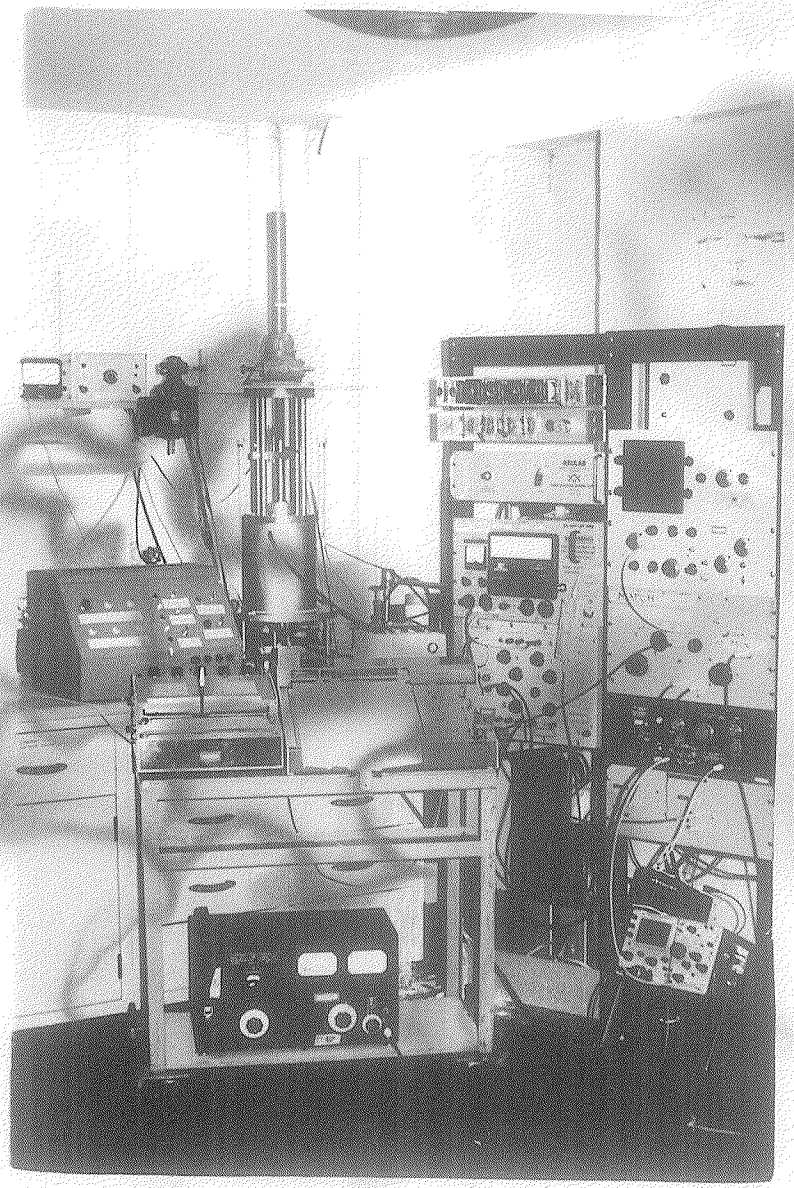

FIGURE 3-1 ABSORPTION DETERMINING APPARATUS

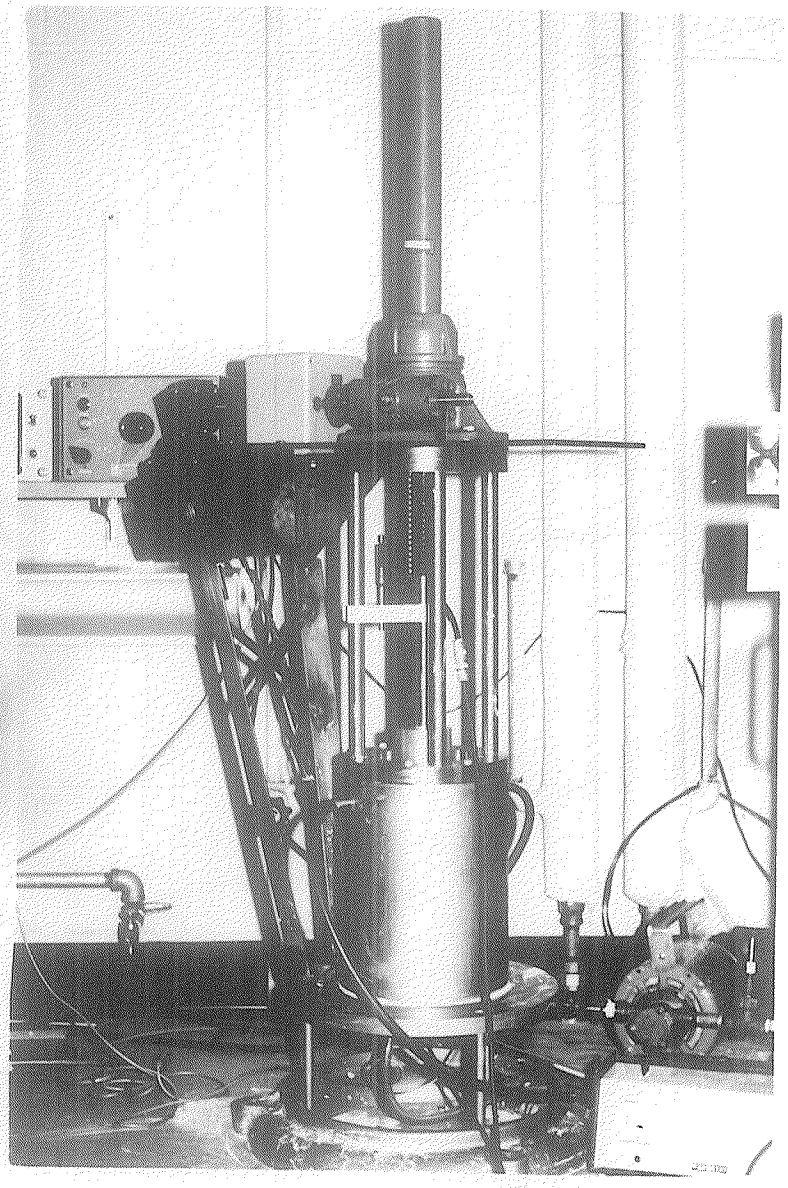

FIGURE 3-2 ABSORPTION CHAMBER

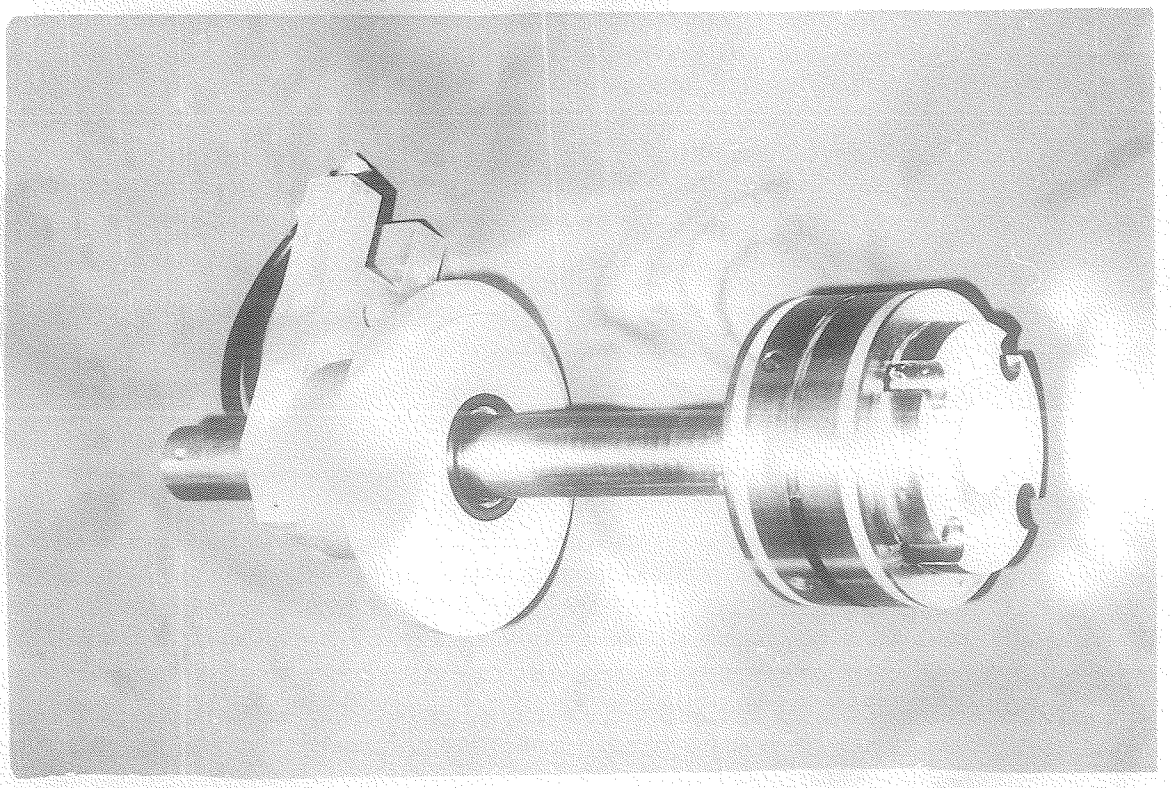

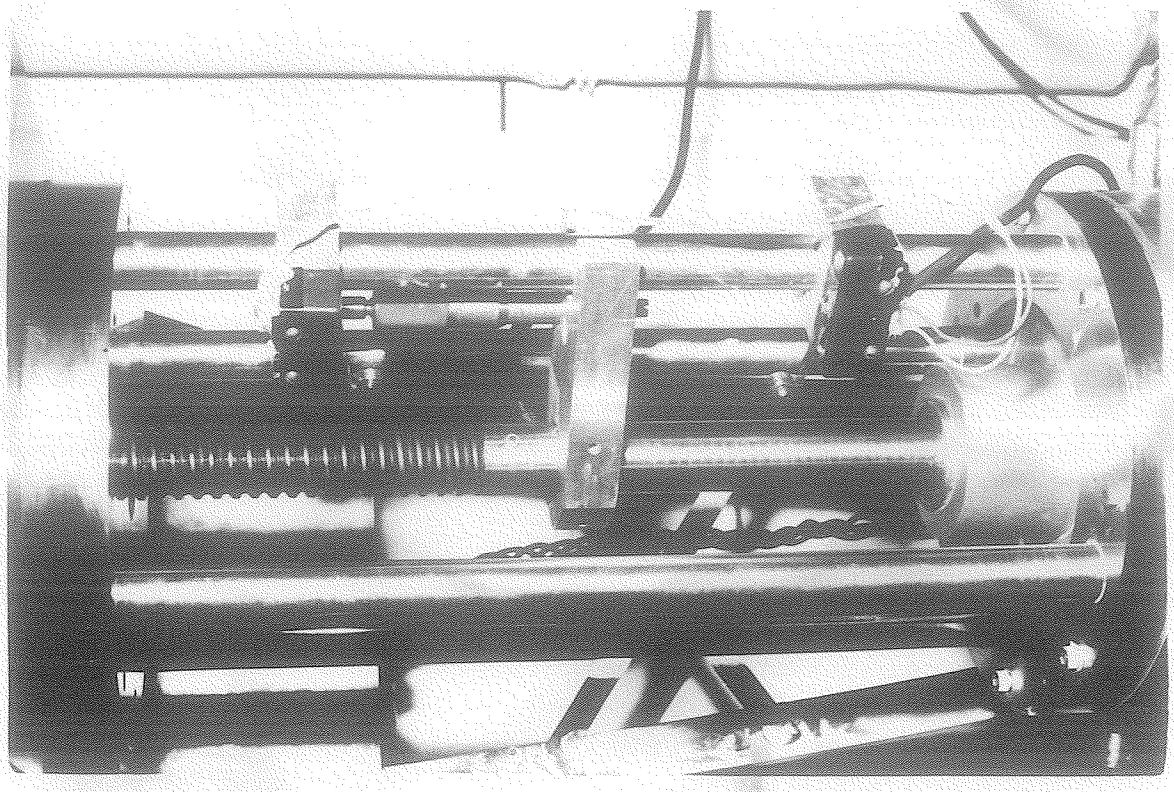

FIGURE 3-4 PISTON ASSEMBLY (LI) CONFIGURATION

FIGURE 3-3 DETAIL OF ACTUATOR - PISTON ROD JUNCTURE. SHOWING ANTIROTATION GUIDE AND REMOTE SWITCHES.

the axis of the piston head accomodates the piston rod. A counter-bored recession along the exterior of this hole receives the transducer housing. The piston head is rigidly fixed in position on the rod by the transducer assembly on one end and an adjustable lock nut on the other.

The transducer housing provides a sealed unit with an rf connector to provide access to the crystal. Contact to the internal crystal electrode is accomplished with a short length of beryllium-copper wire with a small solder bead on the end. The length of the wire is adjusted to be just long enough to provide a stable mechanical contact when the connector is turned tightly into the housing. The solder bead inhibits scratching of the surface electrode.

The upper end of the piston rod is threaded into the lead screw of an actuator unit[1]. The actuator provides transformation of rotary motion to linear displacement via a worm gear and geared lead nut. Reworking of the actuator components was found to necessary to eliminate lateral motion of the end of the lead screw. Additional assurance that lateral forces do not act upon transducer alignment is guaranteed by the use of a bushing at the point of entry into the chamber by the piston. A ball bushing[2] is used so that difficulties with sample contamination by lubricants are avoided. An anodized aluminum housing supports the bushing and permits alignment with the top inside surface of the cylinder, thereby serving the additional function of chamber cover. A rubber seal prevents fouling of the bushing by liquid adhering to the rod. A

small vent provided accomodates a thermometer and also prevents the development of internal pressure.

The actuator is supported fourteen inches above the absorption chamber by four 3/4 inch stainless pillars. Rotation of the lead screw is restrained by a notched aluminum block fixed to the piston rod in such a way that vertical motion is guided by one of these pillars. The aluminum block serves an additional function as support for a micrometer with which small vertical displacements can be accurately measured.

A Bodine 1/25 HP synchronous, four lead, capacitor motor[3] is used to drive the actuator. The motor is reversible and includes an internal gear reducer so that a speed of 180 rpm at 11.4 lb-in. is obtained at the output shaft. Connection to the actuator occurs through a variable speed gear box which permits speed reduction in ten integral ratios from 1 : 1 to 200 : 1. The actuator provides one inch of linear displacement for every ninety-six revolutions of the input shaft so that ten piston speeds between 1.875 in/min to 0.009375 in/min are available.

The direction of the motor is controlled both at a remote panel and by switches that may be mounted optionally on the vertical pillars, activated by the micrometer support (Figure 3-1). The use of these switches permits the operation to be self-cycling over a predetermined displacement.

Rigid mechanical connections couple the motor shaft to the piston rod so that the displacement may represent the

synchronous action of the motor as nearly as possible. The ratio of the output torque to that required to turn the actuator shaft under load condition is about 5 : 1. This load condition was selected to prevent slippage of the armature relative to the driving field.

In the high frequency range a reassembly of components is necessary to provide the additional precision required. Although the piston-cylinder configuration is retained, the guiding surface for the transducer displacement is the precision bored hole in the piston block (Figure 3-6) that is also used for the (LI) frequency range measurements. This block is inverted and placed near the bottom of the chamber.

The transducer assemblies are each composed of a 3/4 in. diameter fused quartz delay rod and associated quartz transducer mounted in a stainless steel housing. Matched transducers, 1.5 in. in diameter, with a fundamental frequency of 15 MHz are employed. The rf connectors are fitted to the housing and electrical contact is made in the same manner as described previously. The housings are machined to provide a precision ($\pm$0.0002 in.) sliding fit for the delay rods which are sealed in place by a thin filet of epoxy resin. Because of the difference of thermal coefficients of expansion between quartz and stainless steel these assemblies are not usable much below room temperature. The lower transducer remains stationary and its alignment is maintained by penetration of the housing through the ball joint and 0.5 in. into the guiding bore.

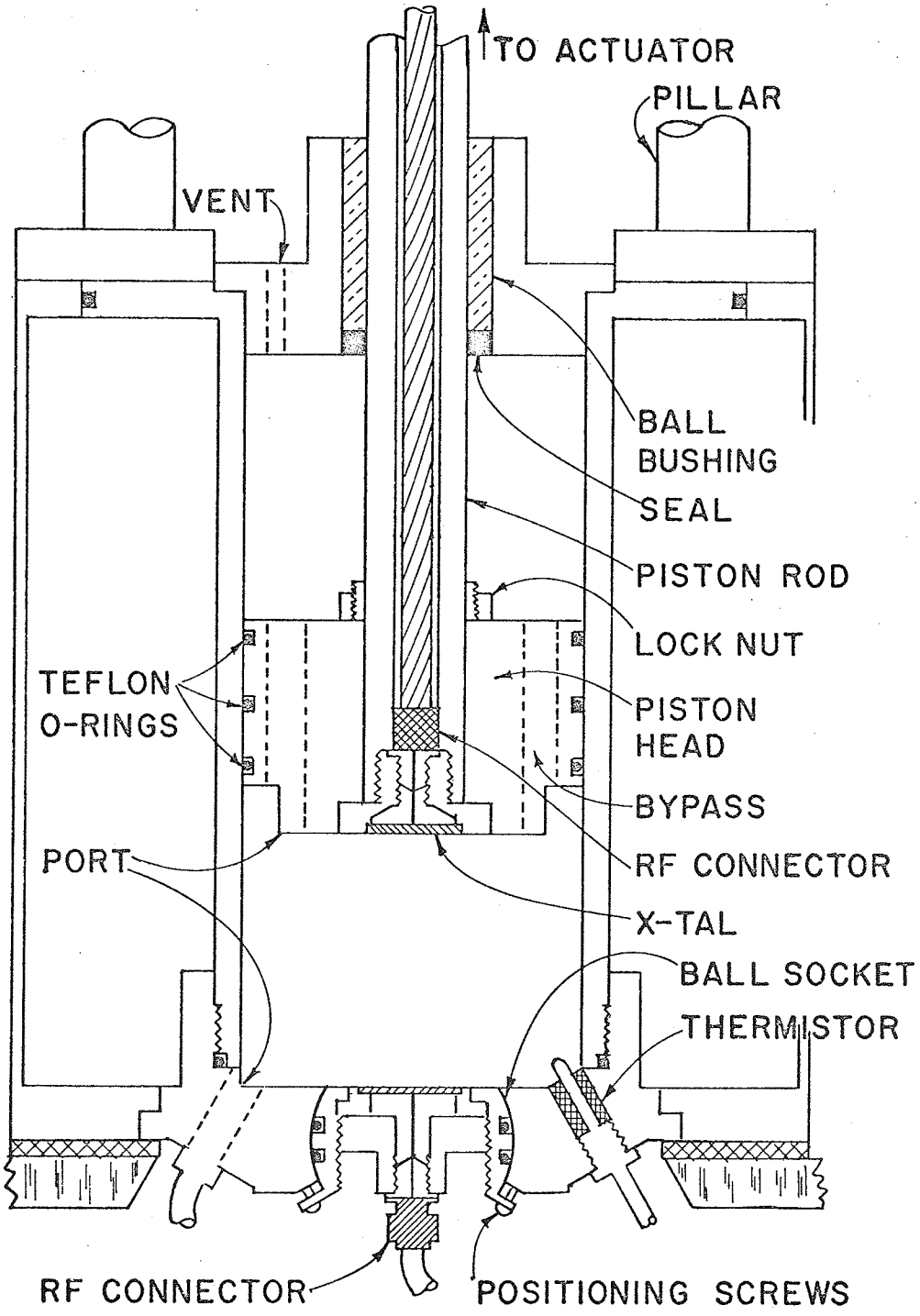


FIGURE 3-5 DETAIL, ABSORPTION CHAMBER (LI) CONFIGURATION

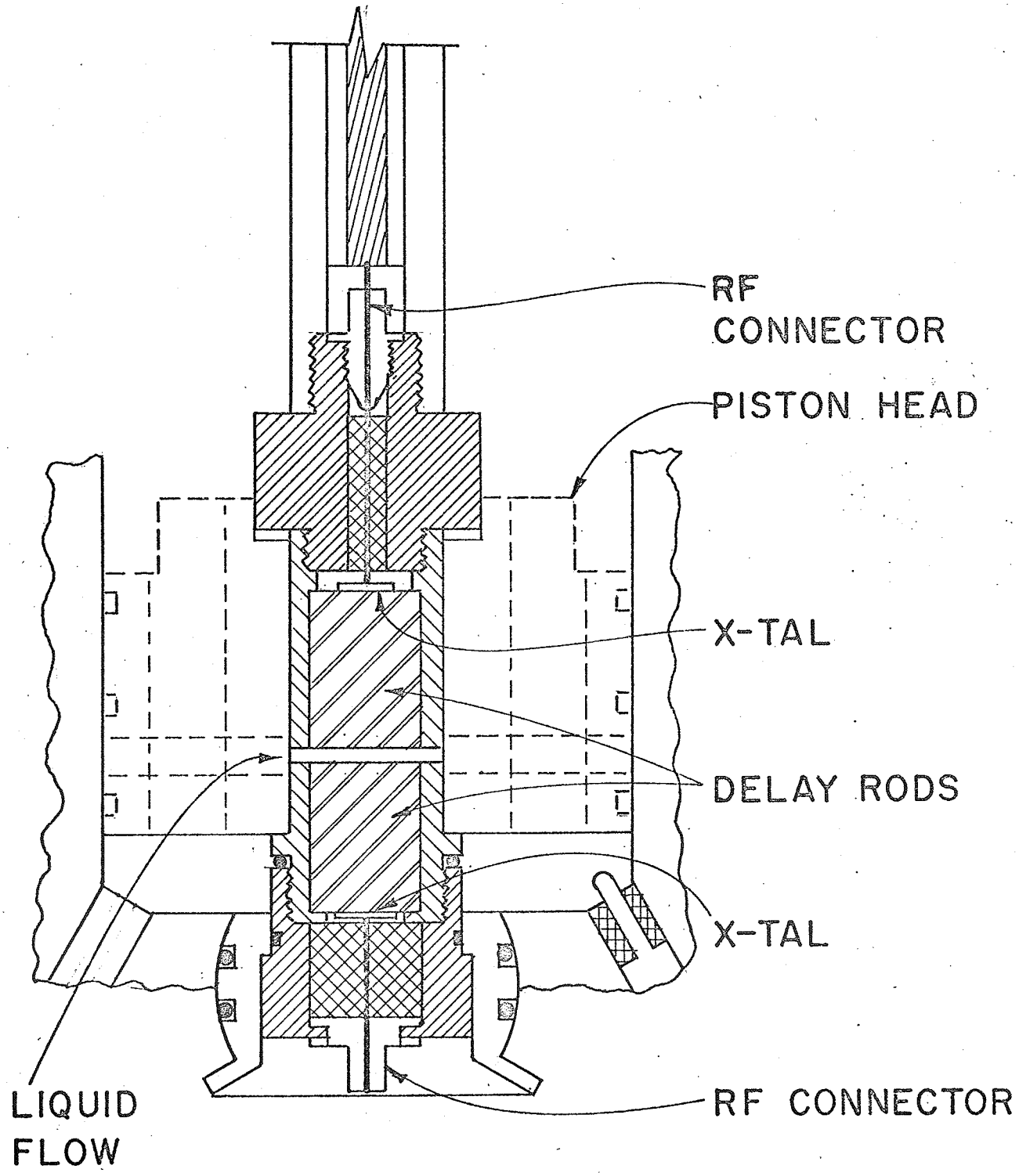


FIGURE 3-6 DETAIL OF (H) CHAMBER CONFIGURATION

The upper transducer housing is driven in the same manner as described above. Smooth translation of the rod is maintained by the use of a single O-ring about the exterior of the housing.

2. Transducers And Transducer Mounting

Optically polished X-cut quartz crystals are obtained in matched pairs (±0.01%) from the Valpey Crystal Corporation, Holliston, Mass.. Mounting of the crystals for the low and intermediate frequency measurements is similar to that described by Carome and Witting (1960). The transducers are edge-supported by a thin annulus of epoxy resin and a narrow (0.005 in.) guide ledge counter-faced into the holder. Chromium on gold electrodes are electro-deposited to the faces of the quartz. With the transducer fixed in the housing, the exposed face is electro-deposited to form a continuous contact to the holder. The 15 MHz transducers are cemented to optical grade, polished, fused, quartz rods also obtained from Valpey Crystal Corporation. The end and cylinderical surface of the delay rod is electro-deposited prior to the fixation of the transducer to provide a contact with the hidden surface of the transducer. A small drop of resin is applied to the rod and squeezed out while wringing the two surfaces together. Satisfactory mating of the surfaces was determined acoustically at 285 MHz using a Matec PR201 Attenuation Comparator. The generation of a suitable bond results in an exponentially decreasing echo pattern with negligible echo deterioration near the baseline. When a good bond is achieved, the crystal

is held in place under pressure with a Teflon die and the assembly cured at 150°C for ten hours.

3. Electronic: Principle Of Operation

Figure 3-7 is a block diagram of the arrangement of the electronic components used for absorption and velocity measurements. The sequence of events begins at the pulsed oscillator with the formation of a rf modulated pulse with a peak to peak amplitude of 10 - 200 volts. The pulse is applied to the quartz transducer via a network that permits the output impedance of the oscillator to be properly matched to that of the crystal. A variable attenuator is inserted between the oscillator and the source in instances when the minimum stable voltage available at the oscillator is too great to be tolerated by the receiver. The ultrasonic pulse is generated, detected and the small resulting rf signal ( < 50mV) is sent to an electronic receiver. At frequencies below 10 MHz, a broadband receiver is used and above 10 MHz a high gain heterodyne receiver is employed. After appropriate amplification, the pulse is detected and rectified so that only the pulse envelope remains for further analysis. This signal is then applied to the input of a coincidence gate. The portion of signal that is allowed to pass the gate is determined by the coincidence in time by a square wave pulse from the pulse generator which is triggered at a variable time after the rf driving pulse. The important feature of this device is that it permits the removal of undesirable events from the signal sequence.

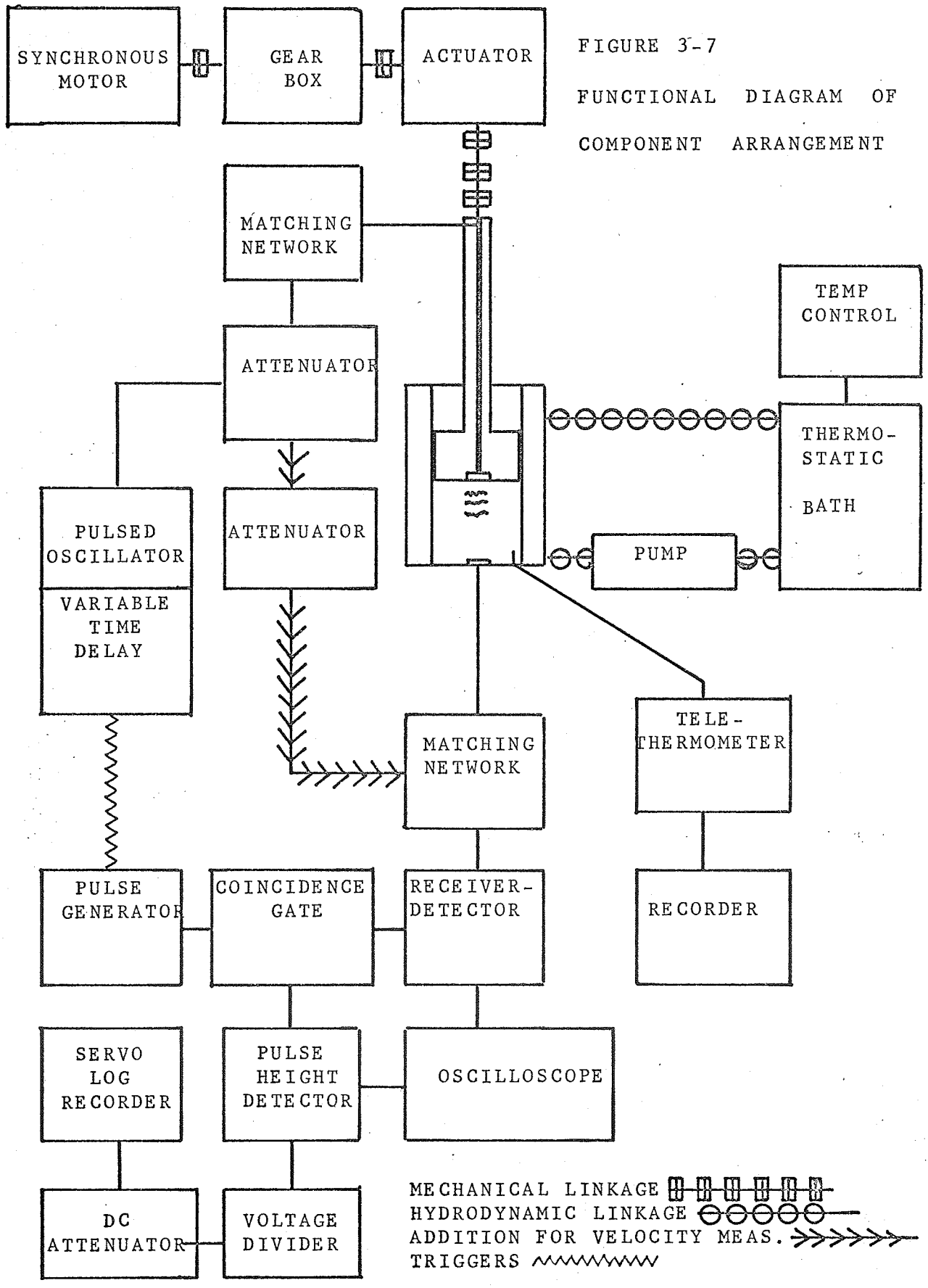


FIGURE 3-7

FUNCTIONAL DIAGRAM OF COMPONENT ARRANGEMENT

Particularly of interest here is the elimination of rf feed-through that may occur. The inclusion of the gate permits measurements at higher frequencies than would normally be possible. By varying the gating pulse length and the time delay, it is possible to "gate out" for analysis all or any portion of the signal train. At low frequencies, where a number of echos are present, the analysis and tracking of any echo is easily accomodated.

The maximum voltage that is allowed to appear at the output of the gate is determined by the amplitude of the gating pulse. Appropriate selection of the pulse voltage makes it impossible to overload subsequent detecting devices. The pulse envelope is next fed to a pulse height detector which produces a dc voltage proportional to the amplitude of the largest pulse in the signal sequency, independent of other repetitive signals that may be present. Thus, when a multiple echo pattern appears at the output of the gate, it is not necessary to track continuously the first echo but merely to remove the rf feed-through. The input to the detector ranges from about 0.2 to 10 V and the voltage gain is -1, so that a fixed dc attenuator is necessary to reduce the signal to a level appropriate ($\sim$50 mV) for the recorder. A servo-logarithmic recorder is employed with a variable dc attenuator at the input. Precise ($\pm$0.01dB) units of attenuation may be inserted here in order to calibrate the recorder scale.

The measurement of the attenuation in a liquid is

accomplished by changing the separation of the transducers at a constant speed so that a straight line is generated at the recorder with slope of $\pm\alpha$ depending on the direction of the displacement.

Pulse lengths from 0.5 to 20 microseconds are employed, depending upon frequency and acoustic path length. For absorption measurements, the criteria that the pulse length be compatible with the band width of the transducer (Nozdrev, 1965) is always observed, i.e.,

$$T < \frac{2}{\Delta f} = \frac{2Q}{f_o}$$

where T is pulse length, Q is the mechanical quality factor, $f_o$ is the center frequency and $\Delta f$ is the bandwidth.

The frequency of maximum acoustic response is determined by a variation of method recommended by Arenberg (1966). A digital counter is used to resolve the frequency of a signal generator signal necessary to produce a zero beat with the received acoustic pulse. It is found that for both sets of transducers the use of maximum acoustic response to determine the frequency of operation is sufficiently accurate ( $\pm$ 0.2%) so that precise determination before each measurement is not necessary.

4. Electronic: Components

PULSED OSCILLATORS: A model PG-650-C pulsed oscillator obtained from the Arenberg Ultrasonic Laboratory, Jamaica Plain, Mass. is employed as the rf modulated pulse source for the range between 3 MHz and 105 MHz. In addition,

this instrument provides the time base and associated trigger pulses for synchronizing the other electronic components for all measurements. Pulse widths are continuously variable from 0.5 to 20 microseconds. Pulse amplitude is adjustable from 0 to about 600 volts into a 93 ohm load and the pulse repetition rate is variable from 50 pps to 2400 pps utilizing the internal triggering circuits. Double pulses can be obtained in phase stable pairs of identical duration and adjustable time separation from 20 to 11,000 microseconds. Both direct and delayed trigger outputs are provided.

For frequencies above 105 MHz, the source of the rf pulses is an Ultrasonic Attenuation Comparator model PR-201 manufactured by Matec Inc., Providence, R. I., (see Chick et al, 1959 for details of circuitry of this instrument). This device contains pulsed oscillators, superheterodyne receiver, and video display circuits for ultrasonic measurements between 1 and 380 MHz. The oscillator provides variable (0 to about 100 volts, peak to peak) amplitude pulses into 50 ohms. Discrete pulse widths of 0.5, 1, and 2 microseconds at a repetition rate of 100 pps are provided by the instrument as supplied from the manufacturer. Longer pulses can be obtained by substituting additional pulse transformers with correspondingly smaller pulse amplitudes. Higher repetition rates are most conveniently achieved by triggering the oscillator externally. Although the PR-201 provides an input for an external triggering mode, it is

found that stable operation is only accomodated by disconnecting the internal triggers. Because of the limitation in pulse length, the Arenberg is the preferred pulse source and is used exclusively below 100 MHz.

ATTENUATORS: Two 50 ohm attenuators with ranges of 0 to 12 dB and 0 to 80 dB manufactured by Daven Div., Manchester, N. H. are employed in situations where 50 ohm terminations are required. Ninety-three ohm attenuators manufactured by Arenberg Labs with a range of 0 to 122 dB are used for corresponding 93 ohm loads. Both types of attenuator have rated uncertainties at $\pm \frac{1}{2}$ dB (1%).

MATCHING NETWORKS: Approximate matching from 3 MHz to 42 MHz is achieved by insertion of a tuned transformer section in parallel with the transducer. By operating the transformer in a partial resonance condition, i. e., resonating either primary or secondary with a shunt capacitance, an appropriate "magnitude" impedance transformation may be accomplished (see for example, p. 435, Everitt and Anner). Rotary air core inductors provide a convenient autotransformer with a continuously variable tap. Either of two transformer sections are used at each transducer to provide matching up to a frequency of about 42 MHz, limited by the self-resonance of the coils. At higher frequencies, matching is accomplished with sections of coaxial cable of various lengths in conjunction with double-stub tuners.

RECEIVERS: A Matec PR 603 broadband untuned receiver is employed at frequencies below 10 MHz. This unit provides nearly 70 dB gain. Above 5 MHz the internal superheterodyne receiver of the Matec PR 201 is used (Chick et al, 1959). This receiver employs a synchronously tuned, four stage 60 MHz i.f. section with a gain of about 80 dB and bandwidth of 1.5 MHz. In order to prevent stray signals generated by the local oscillator from entering the i.f. strip, a variable and a fixed frequency trap are employed at the output of the rf mixer. The variable trap tracks the local oscillator frequency and the fixed trap is set at 65 MHz, the lower limit of the local oscillator. Thus, operation of the receiver is avoided at frequencies where this trap is active (63 MHz).

COINCIDENCE GATE: A simple two transistor, two diode logic module is employed as the gate (Figure 3-8). The emitter-follower ($Q_3$) was included as part of the preliminary design to provide sufficient current gain so that peak rectification techniques of determining pulse amplitude could be investigated. The emitter-follower is not essential when the gate is followed by a high impedance such as that provided by the pulse-height detector described below. Signals with amplitudes between 0 and 10 V are conveniently handled by the gate with a common mode of two positive coincident signals appearing at the output. In addition, the signal of interest is accompanied by a pedestal of about 1 V. The pedestal, which is characteristic

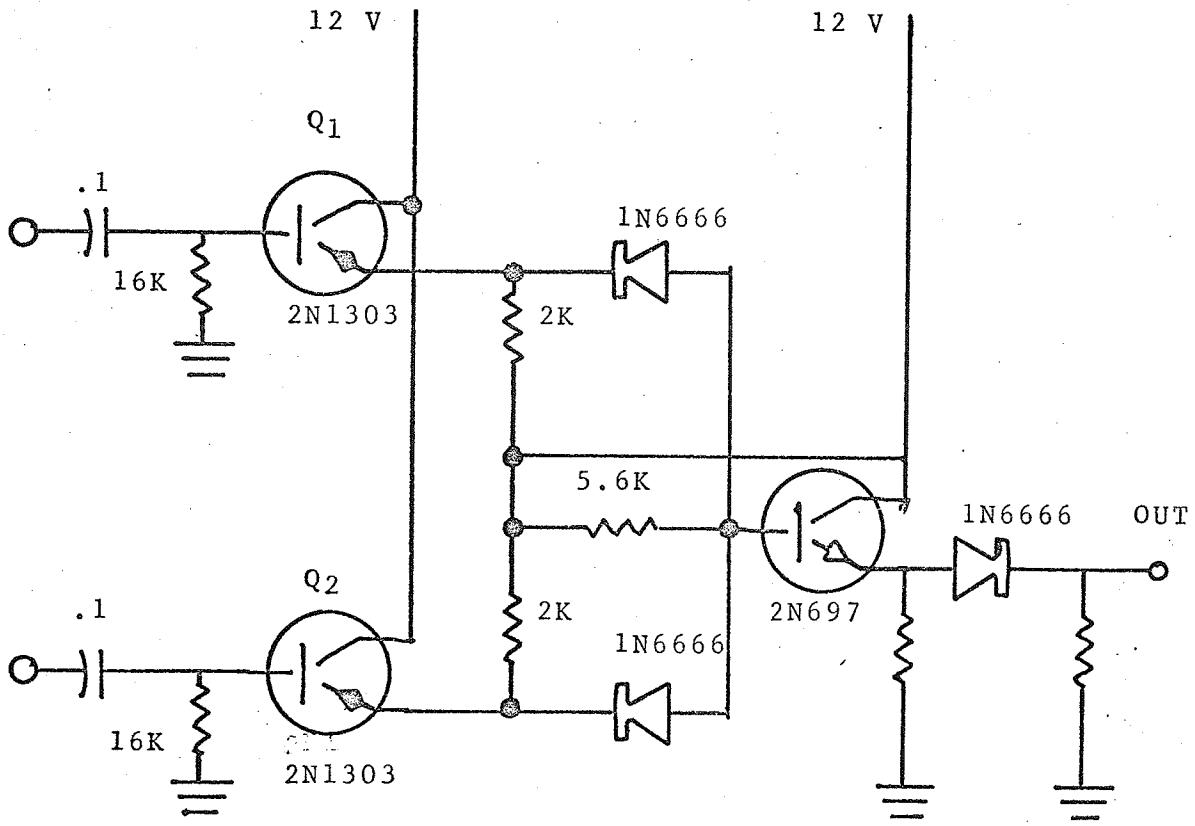


Figure 3-8: COINCIDENCE GATE

of this type of gate, carries the entire signal at sufficiently high potential such that difficulty with threshold devices (diodes, etc.) is obviated at small signal amplitudes.

PULSE HEIGHT DETECTOR: Detailed description of this circuit and its characteristics may be found elsewhere (Sylvan, 1963; G. E. Transistor Manual, 1964). Basically, this is a peak-sensitive operational amplifier which accurately transforms pulse amplitude to dc, utilizing a self-adjusting bias in a tunnel diode threshold sensing element. A high degree of flexibility in circuit parameters is possible. The pulse height detector used in the present investigation has the following characteristics: input impedance, 100 k$\Omega$ ; voltage gain, -1; output ripple voltage less than 40 mV peak to peak; output impedance, 10 k$\Omega$ . The bias current of the tunnel diode is adjusted so that the output voltage is zero when the pedestal voltage of the gate appears at the input.

OSCILLOSCOPE: A Tektronix Type 453 transistorized oscilloscope is employed. This instrument has dual channels each having vertical amplifiers with a dc to 50 MHz bandwidth. For the most part, the oscilloscope is used to monitor the position relationship in the time domain of the various signals. One particularly useful feature is the ability to display the sum or difference of two signals with common mode rejection ratio of nearly 100 : 1 for signals up to 5 MHz. Thus, if one observes the difference

mode of the signal at the input and output of a circuit element, e. g., the pulse height detector, appropriate adjustment of the relative channel gain will produce a null for a linear element. In addition, the dynamic range may be indicated by the dependence of the null on signal amplitude.

PULSE GENERATOR: A Type 1217-C General Radio Co., Unit Pulse Generator is employed as a source for the gating pulse.

RECORDER: The acoustic data recorder is a Sergent Model SRL, which displays the electric potential as a function of time. Conversion of the signal to the logarithmic form is accomplished mechanically with single cycle (20dB) logarithmic gears. Full scale deflection is 24 cm and the maximum balancing speed requires one second for full scale travel. Full scale potential is variable from 1 mV to 120 mV. The chart paper is driven by a three speed synchronous motor at 0.2, 1, and 5 inches per minute. Deviation from a true logarithmic response is of the order of the width of the pen line ($\pm$ 0.03dB). Calibration of the scale is most conveniently achieved by insertion of precisely ($\pm$ 0.01dB) known dc attenuation units at the input of the recorder.

5. Temperature Control And Measurement

Maintenance of constant temperature is achieved by the circulation of water from a 15 liter thermostatic

bath through the annular space about the acoustic chamber. The bath temperature is controlled using a thermistor in conjunction with a temperature controlling unit and a 1,000 watt immersion heater balanced against the circulation of 16°C tap water through a heat exchanger. The control thermistor is imbedded in the bath liquid rather than the sample chamber to avoid large oscillations that result from the high thermal mass of the latter.

A second thermistor sealed in a stainless steel fixture is mounted in the base of the chamber so that the tip extends about ½ inch into the sample. This temperature is monitored by two means: 1) by a meter reading, resistance bridge which allows direct observation of the temperature to ±0.2°C and 2) by a servo recorder which provides a continuous record of the temperature with accuracy of ±0.03°C. Both of these systems are standardized against a National Bureau of Standards calibrated thermometer.

The sample may be continuously mixed by circulation through an external metering pump. Although it is not desirable to remove the liquid from the chamber, circumstances did not permit the inclusion of a somewhat more elaborate internal mixing scheme. Since practically all of the investigations are carried out at temperatures near that of the external environment, this method did not cause a significant loss of stability. It is found that with the above scheme the temperature can be maintained

and determined with an accuracy of $0.01^{\circ}C$ at $20.0^{\circ}C$.

D. Determination Of The Absorption Coefficient

At frequencies above 3 MHz the absorption coefficient is determined directly from the slope of the recorder tracing. In order to correct for diffraction losses, it is assumed that the intrinsic absorption and that due to diffraction are noninteracting and additive (Del Grosso, 1964). In addition, it is found at frequencies above 3 MHz in the suspensions studied that the attenuation attributable to the presence of suspended matter, $\alpha_1$, and that due to the suspending fluid, $\alpha_0$, are also additive (Chapter IV). Thus, the total absorption, appears to comprise three terms, viz.,

$$\alpha_T = \alpha_1 + \alpha_0 + \alpha_D(x)$$

In the solvent $\alpha_1 = 0$ so that

$$\alpha_{T,0} = \alpha_0 + \alpha_{D,0}(x)$$

The diffraction losses at a given point in the suspension, $\alpha_D(x)$, and in the solvent, $\alpha_{D,0}(x)$, will be the same if the wavelengths are identical. It is found in the suspensions investigated that $\alpha_T/\alpha_{T,0}$ increases with concentration more rapidly than the ratio of wavelengths. Typically, at a concentration of 10% it is found that $\alpha_T/\alpha_{T,0} \approx 8\text{-}10$ while the difference in wavelength has changed about 4% (Chapter IV). Thus, by assuming

$\alpha_{D,o}(x) \approx \alpha_D(x)$, the error introduced by this assumption will always be small relative to the total absorption. Therefore,

$$\alpha_I = \alpha_T - \alpha_{T,o}$$

and the curve obtained by subtracting the absorption tracing in water from that in the suspension will yield the desired parameter.

## E. Velocity Measurements, Tracking Error, And Temperature Stability Characterization

In the early stages of this work, velocity was determined by measurement of the time delay of an acoustic transient occuring in a sample of known thickness (Pellam and Galt, 1946). This technique has the intrinsic limitation that group velocity rather than phase velocity is the parameter being examined (Del Grosso, 1964). This difficulty proved to be problematical, however, as the error that arose experimentally ($\pm$ 1%) proved to be more than an order of magnitude greater than those introduced when dispersion is neglected. A more interesting technique was discovered in the course of investigation which permitted a somewhat more accurate measurement of the velocity as well as characterization of tracking errors (deviation from linear correspondence between piston displacement and paper movement) and temperature stability.

The arrangement of the electronic and mechanical components is basically the same as that for the low and

intermediate frequency absorption measurements. An additional attenuator provides a direct rf path (see Figure 3-7) from the oscillator to the receiver. The oscillator is operated in a double pulsed mode with the time delay between pulses adjusted to be nearly equal to the time required for the acoustic pulse to complete a transit in the absorption cell. If this condition is satisfied, the first pulse traveling through the absorption chamber will arrive at the receiver input at the same instant in time as the delayed pulse through the shorting attenuator (Figure 3-9). If the amplitudes are equal, the resulting phase interaction in the region of overlap is such that a null is produced whenever the difference in phase angle $\delta$ between the rf modulations is $180^{o}$. The relative phase is directly determined by the delay of the acoustic pulse in the sample such that phase cancellation occurs whenever the transducer separation is varied through one wave length. Thus, by using the recorder to depict the phase interaction, an interference pattern is generated as the piston is driven through the sample (Figure 3-10). Since the acoustic wavelength in the medium is constant, any nonuniformity in the distance between minima represents the inaccuracy in the tracking system. The velocity is then determined from the knowledge of wavelength and frequency to an accuracy limited by this nonuniformity only.

If the pulse height detector is to be used to detect the null for purposes of automatic recording, it is essential that the non-zero components of the signal be removed. This

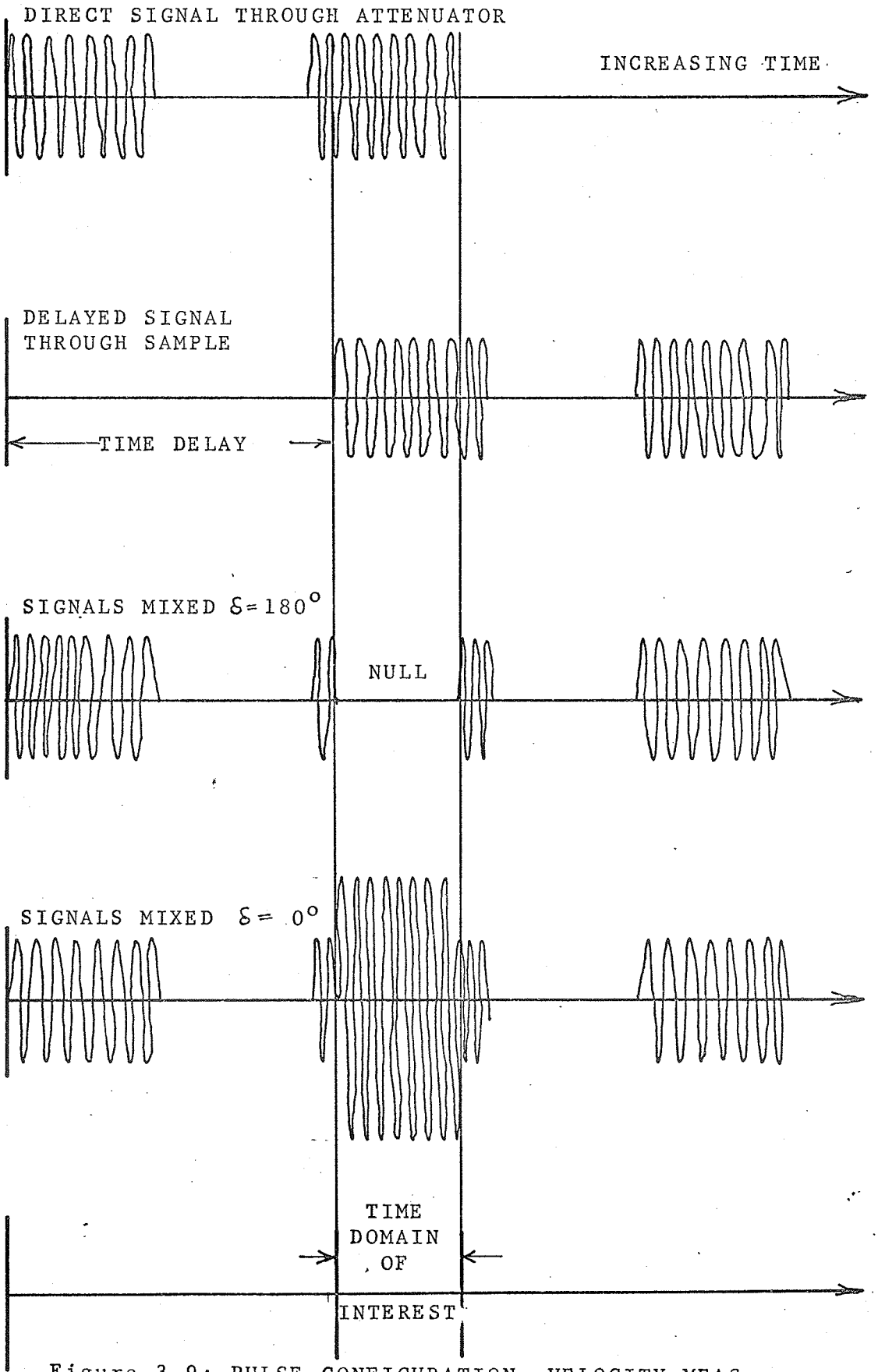


Figure 3-9: PULSE CONFIGURATION; VELOCITY MEAS.

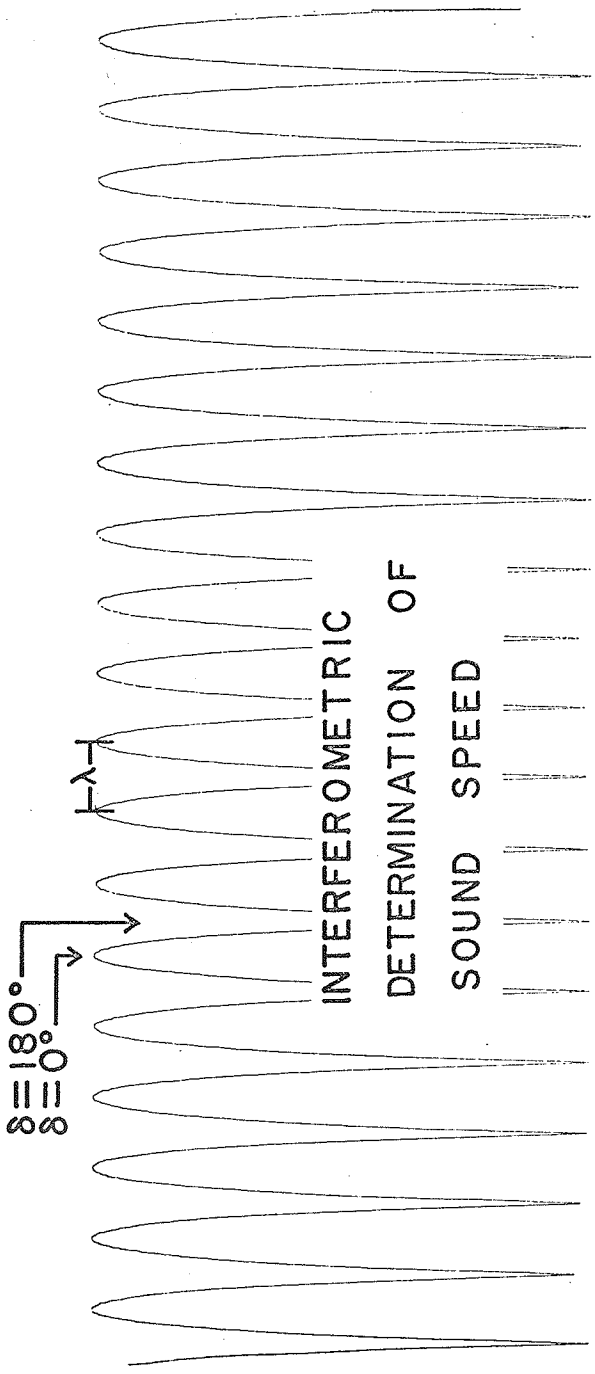


FIGURE 3-10: INTERFEROMETRIC DETERMINATION OF SPEED OF SOUND IN WATER; RECORDER TRACING, REDUCED TO ONE-THIRD ACTUAL SIZE.

is accomplished in the same manner as for absorption measurements. An additional variable time delay, however, is required to control the time position of the delayed rf pulse from the oscillator. The Arenberg pulse oscillator, which is employed for these measurements, permits a maximum pulse length of about 20 microsecond. At 3 MHz this allows a 60 cycle pulse to be used. Ideally, one would like to examine the interference of two long pulses over a large number of cycles. At 3 MHz a compromise is necessary between the length of the overlap and the number of nulls examined. A 30 cycle overlap is used over about 30 cycles. Interferometric patterns up to 21 MHz have been produced in the present instrument. Above 9 MHz, however, jitter in the relative time and phase between the two pulses produced at the oscillator becomes comparable to a cycle so that the sharpness of the null becomes impaired. The extent of the jitter, estimated on the basis of the interference pattern, is found to be less than a quarter of a cycle at 15 MHz or about 15 nsec. Stability of this magnitude is representative of that which can be achieved with a double pulsed system.

The use of a gated amplifier in such a way that the acoustic pulse is mixed with the modulating rf is better suited for this technique. Since a portion of a continuous rf signal is compared to itself, problems with pulse jitter and finite overlap could be, to a large extent, eliminated. The present oscillator does not include this facility, and this particular aspect of the experimental technique was not

pursued further.

The use of the instrumentation as an interferometer allows the investigator to determine accurately the error encountered when the recorder is assumed to be an accurate transducer of piston displacement. In the course of velocity determinations, measurements were made a 3 MHz and over several wavelengths so that the error introduced by the finite width of the null is minimized. By variation of speed reduction, it is possible to separate the contributions to the error by the actuator from the gear box-motor combination. The acoustic system was thus found to have a distance uncertainty associated with it of approximately 3.5 parts per thousand. Virtually all of this uncertainty was attributable to the actuator. Additionally, it is found that the error is introduced as a complex oscillatory deviation with a period corresponding to about 3 cm.

Since the velocity of sound in aqueous liquids has a relatively high temperature coefficient, the interferometric technique described above allows a means for characterizing the temperature stability of the system. One may question the advantage of making such a determination when means for thermistor measurement of temperature has already been provided. The justification resides in the fact that the acoustic method is a reflection of the average temperature of a large volume of medium where as the thermistor is representative of a single point only. The technique is as follows. With the acoustic path length set at a fixed

distance, the phase difference of the interfering pulses is adjusted so the dependence of the recorder response on wavelength is maximal. This occurs at a phase difference of $120^{o}$. The deviation in time of the recorder pen from this initial position is representative of the maximum temperature deviation. The sensitivity of this technique is limited by the phase stability of the oscillator ($\sim$15 nsec). Using water ($20.0^{o}$C), the dependence of velocity on temperature is about 3.5 m/sec/$^{o}$C (Nomoto, 1958). At 9 MHz it is found that a phase change corresponding to 30 nsec is easily detected. The velocity of sound is nominally about $1.5 \times 10^{5}$ cm/sec or $1.5 \times 10^{-4}$ cm/nsec. A path length of 15 cm results in a transit time of $10^{5}$ nsec. A $1^{o}$C change in temperature results in 250 nsec change in transit time. Thus, under these conditions $\pm$ $0.1^{o}$C deviations are easily monitored.

## F. Experimental Error

The error that arises in the determination of the absorption coefficient is usually assessed by comparing values obtained in an extensively characterized liquid for which published values exist. For purposes of this investigation, water is used as a standard liquid. The instrument has been repeatedly checked with distilled water resulting in the accumulation of a large amount of data. It is instructive to compare these results with the accepted values of Pinkerton (1947, 1949) and their implications with regard to system error.

The absorption as a function of temperature for

three frequencies is compared with the accepted behavior (Figure 3-11). The lowest equilibrium temperature provided by the temperature control system is 17.7°C. Although lower temperatures are accessible by the addition of ice to the thermostatic bath, the lack of temperature control and the instability of the acoustic signal made analytical measurements at low temperatures unfeasible. The highest temperature at which this system has been operated is about 60°C. Although acceptable performance is encountered at this temperature, the use of higher temperatures was not pursued to avoid damaging the absorption chamber. In particular, it was feared that the epoxy resin supporting the transducer would deteriorate.

The frequency-free absorption between 17.7°C and 55°C at three frequencies shows some deviation from the accepted values but the general temperature dependence is reproduced. Each point represents the mean value of ten consecutive determinations and all measurements are made with the (LI) configuration of the cell.

Most measurements were conducted at 20.0°C. The results of a large number of measurements of the absorption in water at 20.0°C are tabulated in Table 3-2. Because a smaller number of determinations at each frequency are used in the actual measurement of experimental liquids, the standard deviations and the fractional standard deviations are used to characterize the experimental reproducibility. It is seen that systematic deviation from the Pinkerton

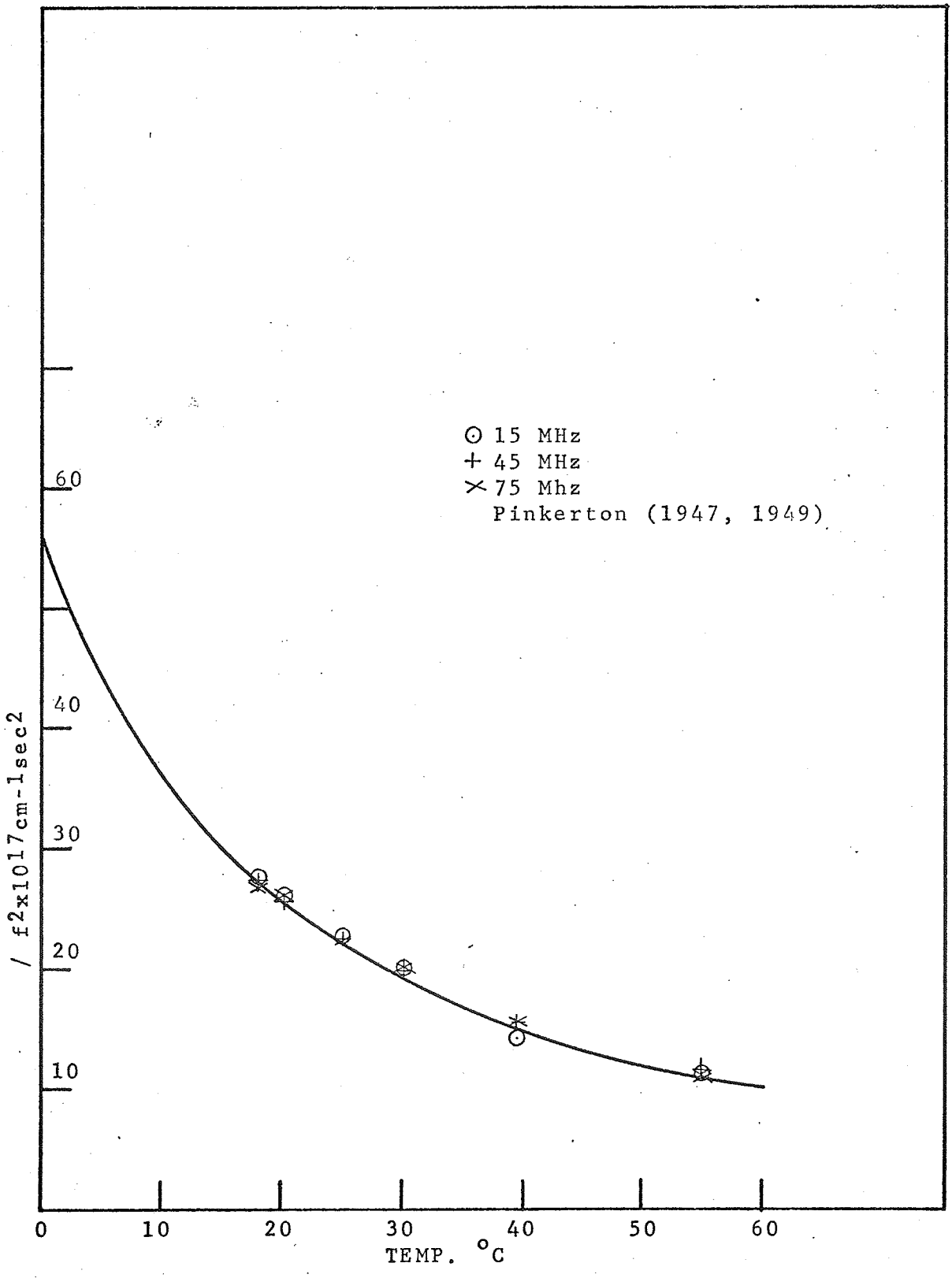


Figure 3-11 Absorption vs Temperature, $H_2O$

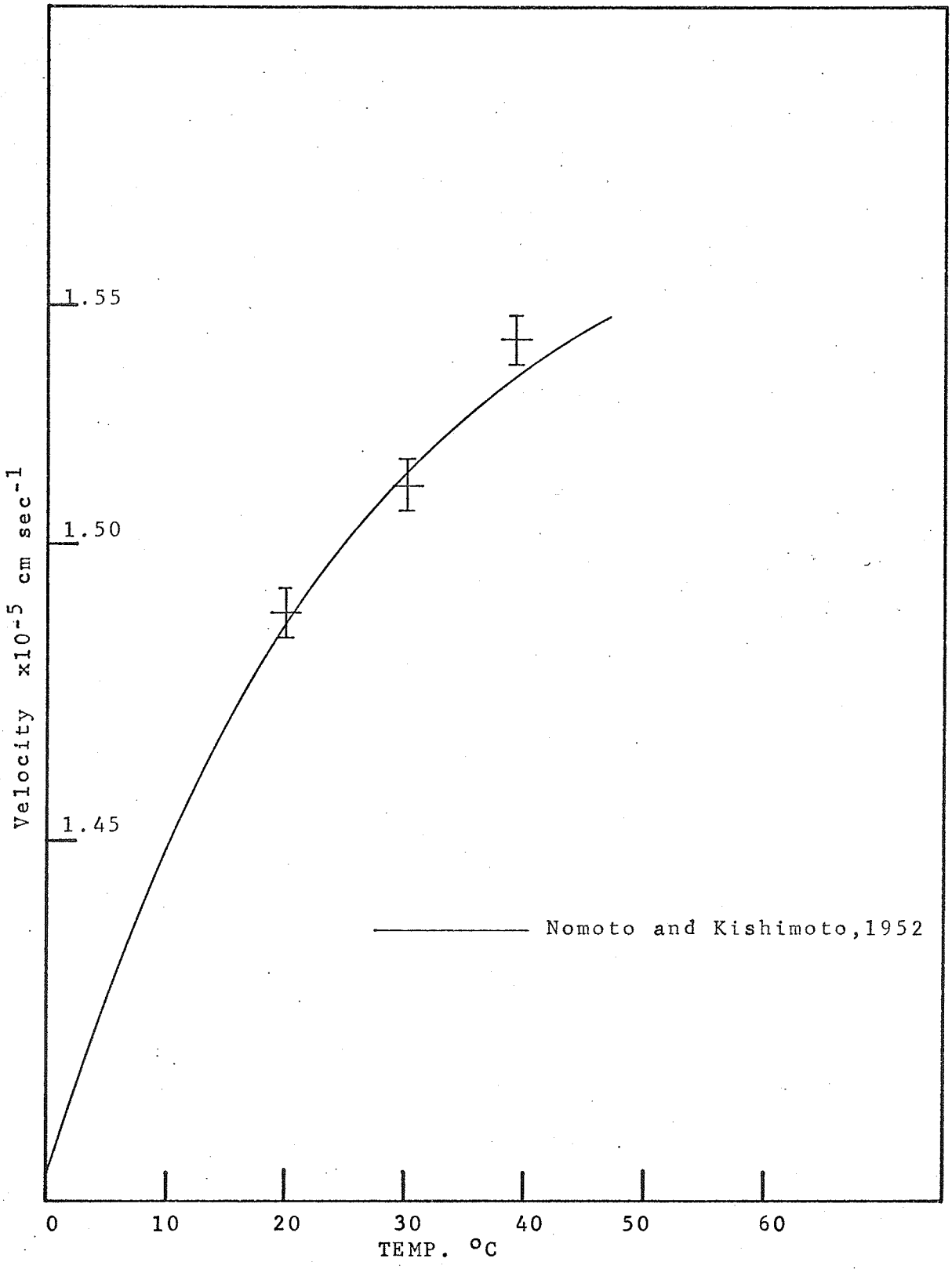


Figure 3-12 Speed of Sound in $H_2O$, 3 MHz

TABLE 3-2

ERROR DATA

SYSTEM PERFORMANCE: WATER 20.0°C

| f MHz | SYSTEM | $\alpha/f^2$ $cm^{-1}sec^2$ | STD. DEVIATION $cm^{-1}sec^2$ | FRACT. STANDARD DEVIATION % | NUMBER OF MEASUREMENTS |
|---|---|---|---|---|---|
| 9 | LI | 27.09 | 1.01 | 3.72 | 68 |
| 15 | LI | 25.87 | 0.84 | 3.24 | 76 |
| 21 | LI | 25.63 | 0.63 | 2.46 | 32 |
| 27 | LI | 25.67 | 0.77 | 2.99 | 77 |
| 33 | LI | 25.25 | 0.72 | 2.85 | 11 |
| 37 | LI | 26.08 | 1.06 | 4.06 | 68 |
| 45 | LI | 25.83 | 1.18 | 4.56 | 45 |
| 51 | LI | 26.33 | 1.18 | 4.48 | 82 |
| 75 | LI | 26.11 | 1.46 | 5.59 | 37 |
| 87 | LI | 26.83 | 1.76 | 6.56 | 4 |
| 105 | H | 26.03 | 1.02 | 3.92 | 37 |

TABLE 3-2 cont'd

| f MHz | SYSTEM | $\alpha/f^2$ $cm^{-1}sec^2$ | STD. DEVIATION $cm^{-1}sec^2$ | FRACT. DEVIATION % | NUMBER OF MEASUREMENTS |
|---|---|---|---|---|---|
| 135 | H | 25.88 | 1.33 | 5.14 | 41 |
| 165 | H | 26.22 | 2.03 | 7.74 | 23 |
| 195 | H | 27.11 | 4.88 | 18.00 | 12 |

ESTIMATED ERROR IN OTHER PARAMETERS:

| | % ERROR |
|---|---|
| FREQUENCY | 0.2 |
| VELOCITY | 0.35 |
| CONCENTRATION (DEXTRAN) | 0.5 |
| CONCENTRATION (POLYSTYRENE) | 0.3 |
| DENSITY | 0.1 |

value ($25.3 \times 10^{-17} cm^{-1} sec^2$) occurs. This may be the result of a systematic error and some difference in the water used.

Also notable is the 4% fractional deviation that exists at 9 MHz. This is presumably due to diffraction losses and experimental values are corrected by this amount where appropriate. The general performance at high frequencies deteriorates with both configurations. Although the (H) configuration never achieves the reliability of the (LI) system, it does allow the continuation of acceptable measurements to about 165 MHz. The results at 195 MHz represent two sets of determinations made at an early and at a late stage in the investigation. While earlier measurements indicated that perfectly acceptable results could be obtained at this frequency with moderate care, the later determinations include a somewhat larger error. This is presumably due to attrition of the bearing surfaces. In addition, it is felt that all the high frequency measurements are to some degree influenced by this effect. However, since most of the data concerning water are not dated, further characterization is not possible.

Without attempting further to resolve the systematic deviation from the Pinkerton value, an $\alpha$ at 20.0°C of $26.0 \times 10^{-17} cm^{-1} sec^2$ is used in all further computations. In the light of the above data, it is not felt that the error introduced by this assumption will be significant.

Because water is in all cases the lowest absorbing material studied, brief consideration of the influence

of the absorption coefficient on error is warranted. For all the materials studied (with one exception) the frequency-free excess absorption decreases with increasing frequency and above 50 MHz a relatively small variation of absorption from that of the solvent is observed. At low frequencies, the excess frequency-free absorption may become appreciable. In all circumstances, however, this has the effect of decreasing the relative magnitude of the losses attributable to diffraction. In general it is felt that the values appearing in Table 3-2 are representative of the maximum error associated with the instrument.

A list of estimated error values that arise in the computation of acoustic parameters is also shown in Table 3-2.

## G. Materials and Methods

WATER: Singly distilled water obtained from the laboratory still was employed in the preparation of all solutions and also for instrument characterization. Deuterium oxide (99.5%) was obtained from the Columbia Organic Chemical Co., Columbia, South Carolina.

DEXTRAN: The dextran was obtained in a fractionated and characterized form from the Pharmacia Fine Chemical Co., Piscataway, New Jersey. The weight and number of average molecular weights as well as the intrinsic viscosity of each fraction was supplied by the manufacturer (Table 3-3). No further characterization was attempted other than determination of the intrinsic viscosity as a check on the manufacturer's values, wherein excellent agreement ($\pm$ 0.5%)

TABLE 3-3

DEXTRAN: Pharmacia Fine Chemical Company

Source: Leuconostoc mesenteroides, NRRL-B512

| $\overline{M}_w \times 10^{-3}$ | $\overline{M}_n \times 10^{-3}$ | $[\eta]_o$ dl/g | $\overline{M}_w/\overline{M}_n$ |
|---|---|---|---|
| 11.2 | 5.70 | 0.098 | 1.97 |
| 21.8 | 14.5 | 0.147 | 1.50 |
| 39.8 | 25.6 | 0.198 | 1.55 |
| 72.0 | 40.5 | 0.256 | 1.77 |
| 167.0 | 105.0 | 0.38 | 1.59 |
| 370.0 | 185.0 | 0.50 | 2.00 |

Other Properties (Granath, 1958)

Partial specific volume $\overline{V}$ : 0.61 cc/g

Statistical segment length ($\overline{M}_w = 10^5$), 8.8 Å

$$2.43 \times 10^{-3} \overline{M}_w^{0.42} \text{ dl/g}$$

Hydrodynamic radius, $R_h \simeq 0.32 \overline{M}_w^{0.50}$ Å

BOVINE SERUM ALBUMIN: Sigma Chemical Company

Properties in 0.1 M KCl (Tanford and Buzzell, 1956)

$M_w$ : 65,000

$\overline{V}$ : 0.734 cc/g

R : 33.7 Å

TABLE 3-3 cont'd

LATEX PARTICLES: Dow Chemical Company

| Radius $\times 10^4$ cm | Standard Deviation $\times 10^4$ cm | Number of Measurements | Comments |
|---|---|---|---|
| .044 | .004 | 1164 | Monodisperse |
| .110 | - | - | Distribution |
| .178 | .003 | 655 | Monodisperse |
| .504 | .003 | 106 | Monodisperse |
| 3 - 7 | - | - | Distribution |

Partial specific volume : 0.95 cc/g (Cheng and Schachman, 1955)

was observed for all samples used in this investigation. Tabulation of the weight average molecular weight $\bar{M}_w$ , number average molecular weight $\bar{M}_n$ , and intrinsic viscosity $[\eta]_o$ , are found in Table 3-3.

The dextran is produced by Pharmacia from Leuconostoc Mesenteroides, strain NRRL-B512. The hydrodynamic properties of aqueous solutions of this material have been studied by Granath (1958), who finds that the statistical segment length is not much larger than the diameter of the glucose molecule (8.8Å vs 5.15Å at a $\bar{M}_w$ of $10^5$) indicating that dextran molecules are highly flexible.

Enough polysaccharide is dissolved in distilled water to form a one liter stock solution with a concentration of 10 - 15%. Solutions are sterilized and clarified by filtering through membrane filters (pore size, 0.3$\mu$) and then refrigerated at 5°C until acoustic measurements are made.

Generally, a small amount of distilled water remains in the absorption vessel as a residue from the preliminary performance check. Thus, the polysaccharide concentration is most effectively determined after the solution has been introduced into the acoustic chamber and vigorously pumped through the vessel for several minutes.

Concentration of aqueous dextran solutions is conveniently determined polarimetrically with an error not exceeding 1%. The specific rotation $[\alpha]_D^{20}$ was determined to be 199°. This compares to a value of +198° by Senti et al (1955) and 199° listed by Pharmacia. A Rudolf model 70 polarimeter capable of resolving ±.01° was employed for optical rotation

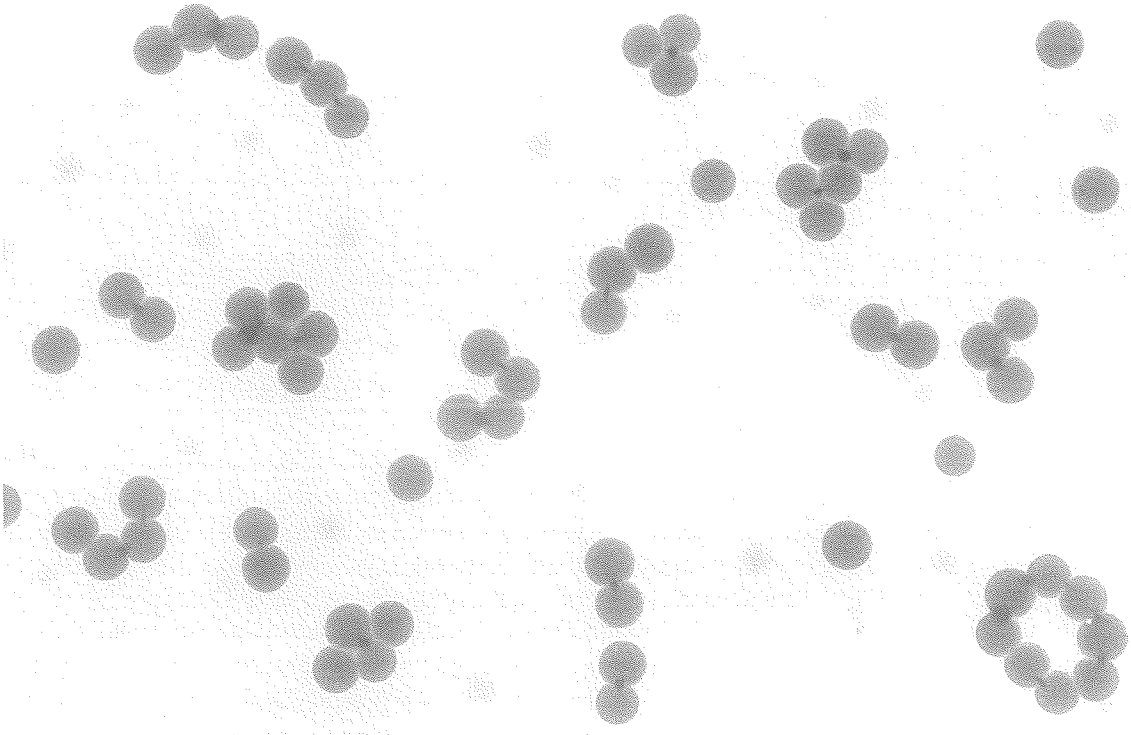

FIGURE 3-13 ELECTRON MICROGRAPH, POLYSTYRENE PARTICLES
RADIUS: 0.044 micron

FIGURE 3-14 OPTICAL MICROGRAPH, COPOLYMER PARTICLES
AVERAGE RADIUS: 3.5 micron

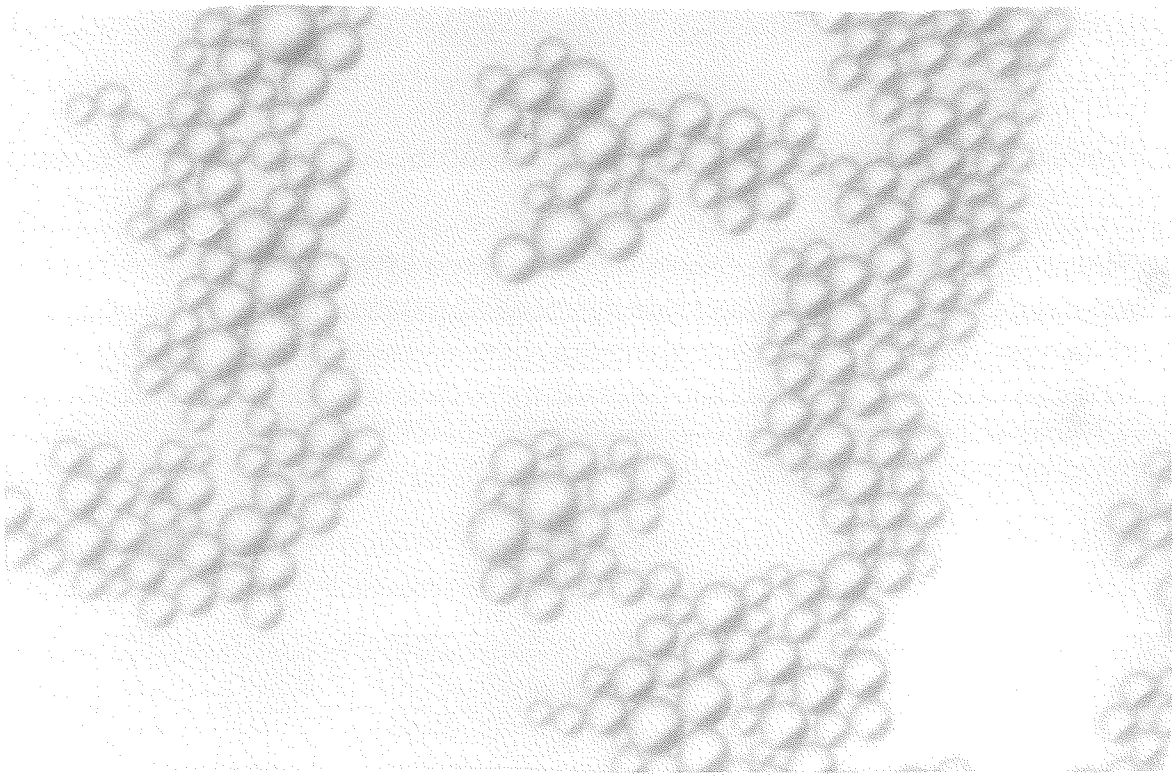

measurements. Room temperature was sufficiently stable ($\pm 1^{o}C$) that no special temperature control was necessary.

Intrinsic viscosities are determined using Cannon-Ubbelohde semi-micro-dilution viscometers suspended in a temperature control bath ($\pm 0.01^{o}C$). The viscometers were selected such that the flow time is all cases was sufficiently long (> 100 sec) to avoid kinetic energy errors. Values obtained agreed with the Pharmacia values in all cases.

BOVINE SERUM ALBUMIN: Fraction V, bovine albumin was obtained from Sigma Chemical Co., St. Louis, Missouri. A one liter solution with a nominal concentration of 10% was prepared by suspending the protein in 0.1M KCl, pH 6.8. This solution was membrane filtered prior to acoustic measurements.

Concentration is determined on the basis of an extinction coefficient of 6.6/g albumin/100mg/cm (Cohn et al., 1947). Observation of the behavior of this material in the ultracentrifuge revealed a single sharply defined peak with a sedimentation coefficient, $S_{20,w}$ equal to $4.07 \times 10^{-13}$sec at a concentration of 5.4 mg/ml. This compares favorably to the accepted value and is a reasonable indication that the material under study is native protein.

POLYSTYRENE LATTICES: Spherical polystyrene and styrene-divinylbenzene copolymer particles suspended in deionized water were supplied by the Dow Chemical Co., Midland, Michigan. Six different dispersions are investigated.

Four suspensions are monodisperse polystyrene lattices,

the type used extensively as a secondary standard in optical and electron microscopy. The sizes of the particles have been characterized accurately by the manufacturer (see Table 3-3). Although these materials are usually only available in 10 ml lots, one liter of each latex was provided through the generous interest of the manufacturer. Particle concentration as supplied in each case is nominally 10% solids by weight.

The other suspensions are heterodisperse. One of these is a styrene-divinylbenzene copolymer latex (DC642-19) with a nominal average particle radius of 3.6$\mu$. The distribution of particle sizes has been characterized by the manufacturer using optical microscopy. The distribution curve is roughly Gaussian with about 99% of the particles having radii between 1.5$\mu$ and 6.5$\mu$. Copolymerization of the styrene with divinylbenzene has the effect of increasing the particle rigidity (Dow Chemical, 1966). This suspension is also supplied with a concentration of about 10%.

The other dispersion investigated is Dow 586 polystyrene latex. This material is a heterodisperse industrial preparation supplied with a concentration of 50% solids by weight. Nominal particle radius is 0.11 micron.

Particle concentration is determined by weighing the residue obtained by evaporating a known volume of suspension to constant weight. Since the polystyrene is very hydrophobic no special drying procedures are necessary.

The concentration of free surface active agent is

determined by centrifuging the particles from a known volume of suspension, membrane filtering the supernatant and weighing the residue that remain after drying. This determination is limited to the suspensions containing the 0.5044 $\mu$ and 3.6 $\mu$ particles. Removing the smaller particles from sufficiently large quantities of suspension (50 ml) is hindered by the small density difference between the particle and water ( $\rho_P / \rho_o \approx 1.05$).

The apparent partial specific volume, $\bar{V}$, of polystyrene latex particles has been determined to be 0.950 cc/g by Cheng and Schachman (1955). In addition, the particles appear to be impermeable to water and thus are not internally hydrated. The density is then given by $1/\bar{V} = 1.052$ which agrees with the value for bulk polystyrene.

Because of the importance of the density, independent determinations were made. Two methods are employed. Assuming impermeability of the particle, the following expression may be derived readily to describe the density of the two component system:

$$\rho_P = \frac{c \rho_T \rho_o}{\rho_o + (c-1)\rho_T}$$

where c is concentration and $\rho_T$, $\rho_P$, $\rho_o$ are the densities of the suspension, particle and suspending liquid, respectively. Using standard pycnometric techniques and allowing an accuracy in measurement of 0.0001 g/cc, the density of all the polystyrene latex particles is found to be in agreement with the previously determined value. The copolymer particles

are also found to have an average density of about 1.052 g/cc. It is found, however, in centrifuging these particles in sucrose solutions that neither complete sedimentation or floatation occurs when the suspending fluid has a density between 1.050 and 1.053 g/cc. In addition, observation of the behavior in a sucrose gradient reveals that while most of the particles accumulate as in a narrow band, isolated particles exist with densities as high as about 1.058 g/cc. This probably is due to some variation of the copolymerization from particle to particle. No further effort was made, however, to characterize the density of this material and the average value will be employed in subsequent discussions.

Contact of the latex with glass and stainless steel results in the deposition of a thin layer of polystyrene. This is avoided to a large extent by treating the contact surfaces with Desicote.

For the most part, the acoustic procedures involved in the use of the particles are the same as with homogeneous materials, with one notable exception. It was found that the piston transducer could not be driven through suspensions of the largest particle size without mechanical seizure due to "wedging" of the particles between the bearing surfaces. This problem can be alleviated by inserting spacers between the transducer housing and piston head so that the transducer may move through the suspension while the piston bears on the surface near the top of the absorption cylinder. This modification, however, limits the maximum transducer separation to the extent that the absorption coefficient and 3 MHz could not

be obtained.

---

1. Manufactured by Duff Norton Corp., Charlotte, North Carolina.
2. Manufactured by Thomson Industries, Manhasset, New York.
3. Obtained from the Minarik Electric Co., Los Angeles, California.

# CHAPTER IV

## RESULTS

The dependence of the absorption coefficient on concentration in aqueous solutions of dextran at 20.0°C for six molecular weight fractions has been measured. Figure 4-1 depicts the behavior at $M_w$ 72,000, which is representative of that observed at all the molecular weights investigated ( 11,200; 21,800; 39,800; 167,000; 370,000). It may be observed that at frequencies greater than 3 MHz a common zero-concentration intercept on the ordinate axis exists which reflects the Stokes $f^2$-dependence of the absorption of the solvent. Thus, by employing a normalized ordinate parameter of $\alpha / f^2$, the data at a number of frequencies are conveniently compared in a single plot. At 3 MHz, the concentration-independent term is removed along with the diffraction losses (Chapter III) so that for this frequency the ordinate is $\Delta\alpha / f^2$. The value of $\alpha$ at each frequency at every concentration represents the mean value of at least five individual determinations.

Effective comparison of the absorption properties of different macromolecular species is facilitated by defining a reduced coefficient that results upon removing the contribution of the solvent and the concentration dependence, viz.,

$$A = \frac{1}{c} \frac{\Delta\alpha}{f^2} = \frac{1}{c}\left[ \frac{\alpha_T - \alpha_o}{f^2} \right]$$

where $\alpha_T$ is the observed absorption coefficient and $\alpha_o$ is the concentration independent term. Figure 4-2 is a composite log-log plot of A as a function of frequency for all molecular weights investigated. The results of measurements of the absorption in aqueous solutions of glucose are also represented. Shear viscosity contributions to the absorption as calculated by the Rouse theory for the highest and lowest molecular weights are depicted within the range of applicability of the high frequency approximation (cf Appendix I). Values of A for the various fractions are shown in Table 4-1. Similar measurements of absorption in aqueous solutions of bovine serum albumin in 0.1 M KCl at 20.0°C are shown in Figures 4-3 and 4-4. The absorption characteristics of aqueous suspensions of beef hemoglobin (Carstensen, 1959b, Edmonds, 1966b) are compared with the albumin data in Figure 4-4. Tabulation of the values of A of serum albumin are also shown in Table 4-1.

The absorption in the five aqueous polystyrene lattices has been measured at 20.0°C in the following concentration ranges.

| R (micron) | Conc. Range (g/cc) |
|---|---|
| 0.044 | 0.0 - 0.1 |
| ~ 0.11 | 0.0 - 0.5 |
| 0.178 | 0.0 - 0.1 |
| 0.504 | 0.0 - 0.1 |
| ~ 3.5 | decreasing 0.0 - 0.1 at 9 MHz to 0.05- 0.01 at 81 MHz. |

In every case, the absorption has appeared as a linear function of concentration to at least 0.1 g/cc. Representative of the dependence of absorption on concentration is that observed in DC-586 (R: $\sim$0.11 microns) in which the concentration range is the greatest (Figure 4-5). The corresponding value of A at each frequency as above is taken from the slope in the concentration range where the dependence is linear. A minimum of three concentrations were used in each case to determine A. A log-log plot of A vs frequency for the lattices is shown in Figures 4-6, 4-7, 4-8, 4-9, 4-10.

The temperature variation of the absorption parameter A, in DC-586 from about 17°C to 48°C at four frequencies from 9 MHz to 51 MHz is shown in Figure 4-11.

The addition of NaCl in an amount sufficient to make a 10% suspension of DC-586 0.05 M in this salt did not result in a detectable change in the absorption properties. Higher concentrations of salt results in flocculation of the latex particles and further variation of the ionic environment of the particle was not attempted. Log-log plots of A vs frequency for the particles investigated are shown in Figures 4-5 to 4-10. A minimum of three concentrations is each case were used to determine the values of A. The theoretical absorption character predicted on the basis of the Lamb, Epstein, Urick relations is shown for reference for each particle size.

In order to further examine experimentally the

importance of the relative motion contribution, it is of interest to investigate the absorption character in the absence of relative motion which is the case when the particle and surrounding medium possess the same density. Since the specific gravity of the particle is fairly close to unity (1.055 at 20.0°C), this situation may be conveniently achieved by employing a $D_2O$- $H_2O$ mixture as the suspending fluid. The results of absorption measurements at 20.0°C in suspensions of 0.504 $\mu$ particles in a $D_2O$-$H_2O$ mexture with a specific gravity of 1.053 are shown in Figure 4-9 along with those obtained with $H_2O$ as the suspending liquid.

Although velocity determinations were not a primary consideration in this investigation, a number of measurements were made using the method described in Chapter III. A composite plot of the relative velocity $V/V_o$, $V_o$ being the velocity of water, for the materials investigated is found in Figure 4-12.

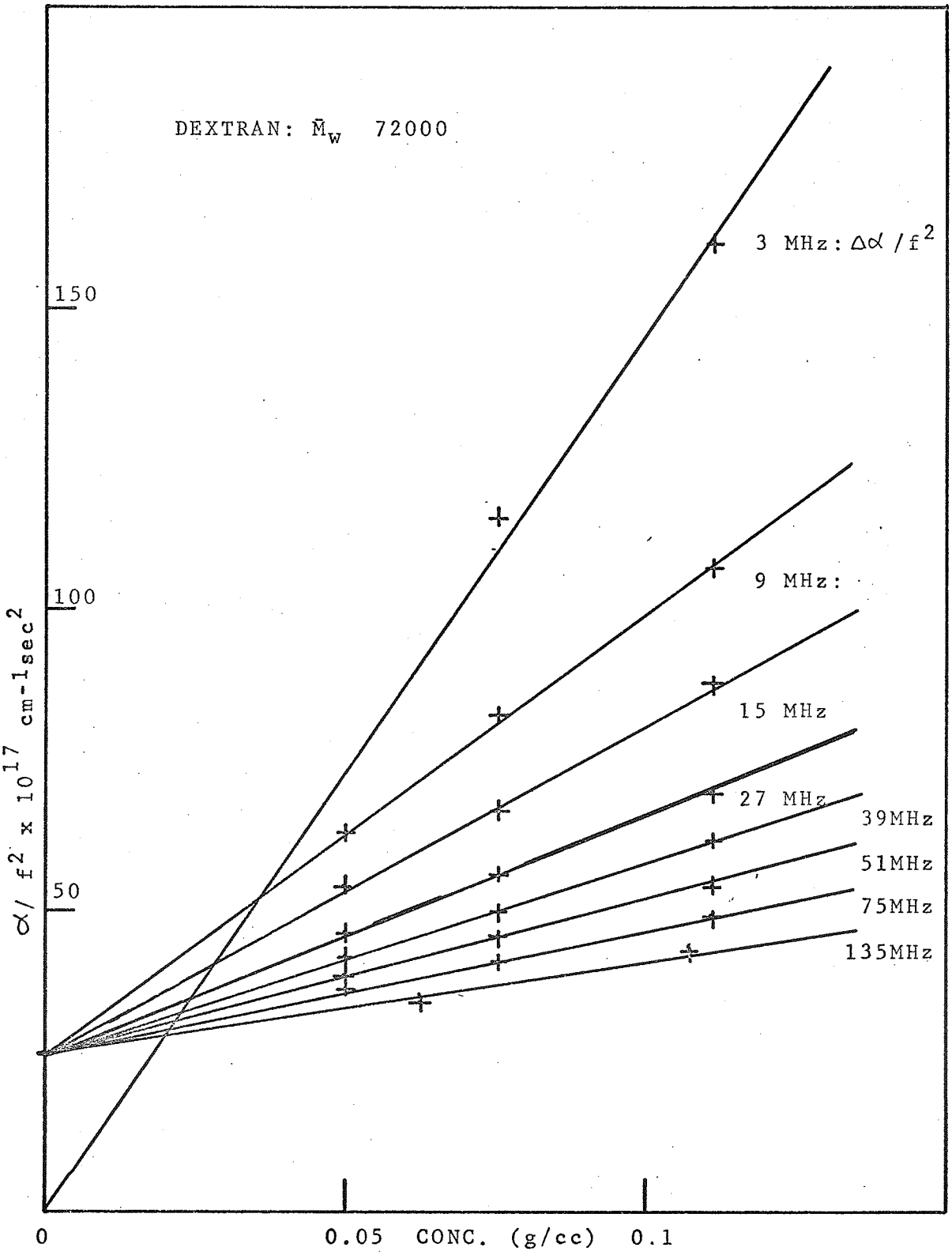


Figure 4-1 Absorption vs Concentration, Dextran $\bar{M}_w$ 72000

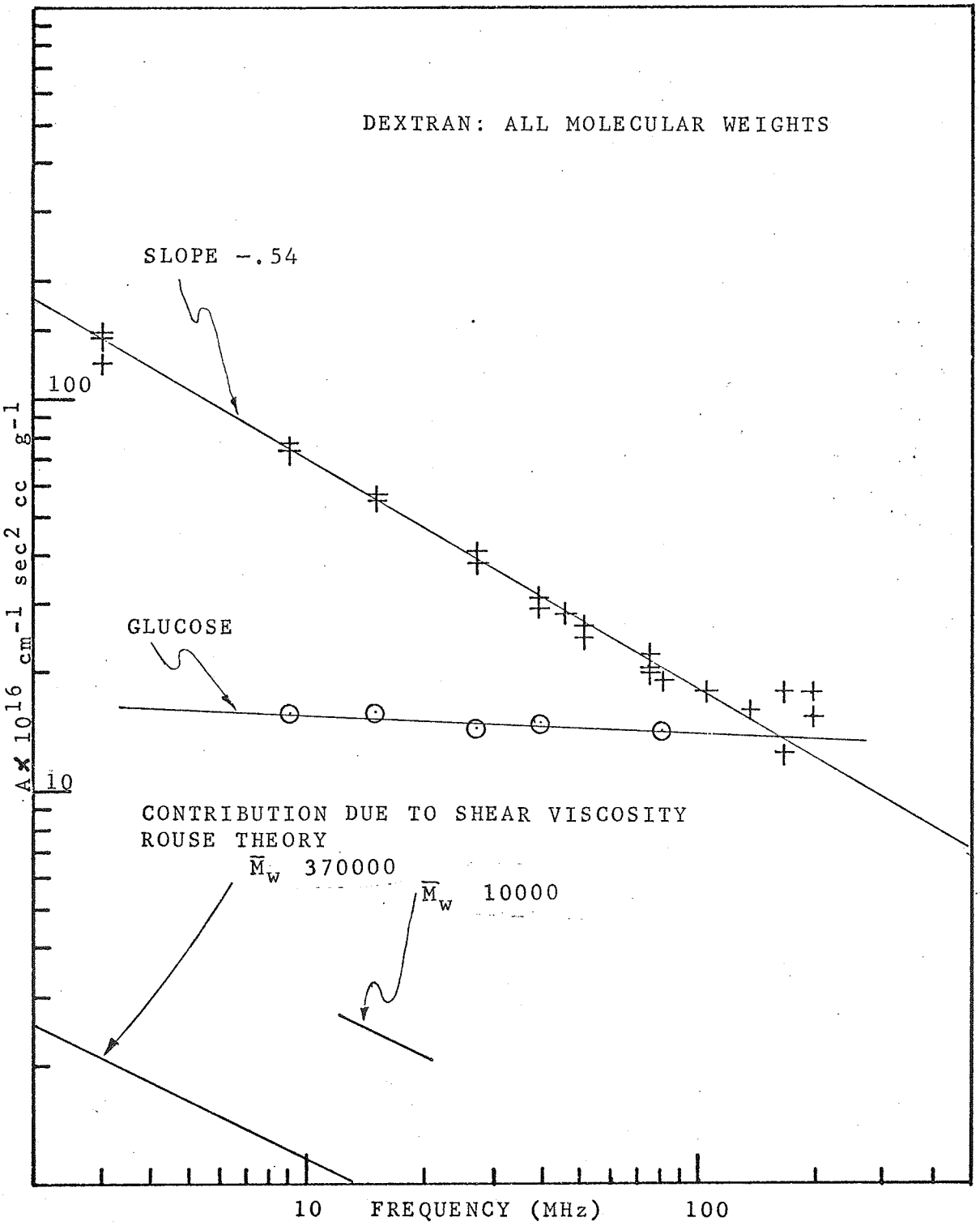


Figure 4-2: EXCESS ABSORPTION IN DEXTRAN

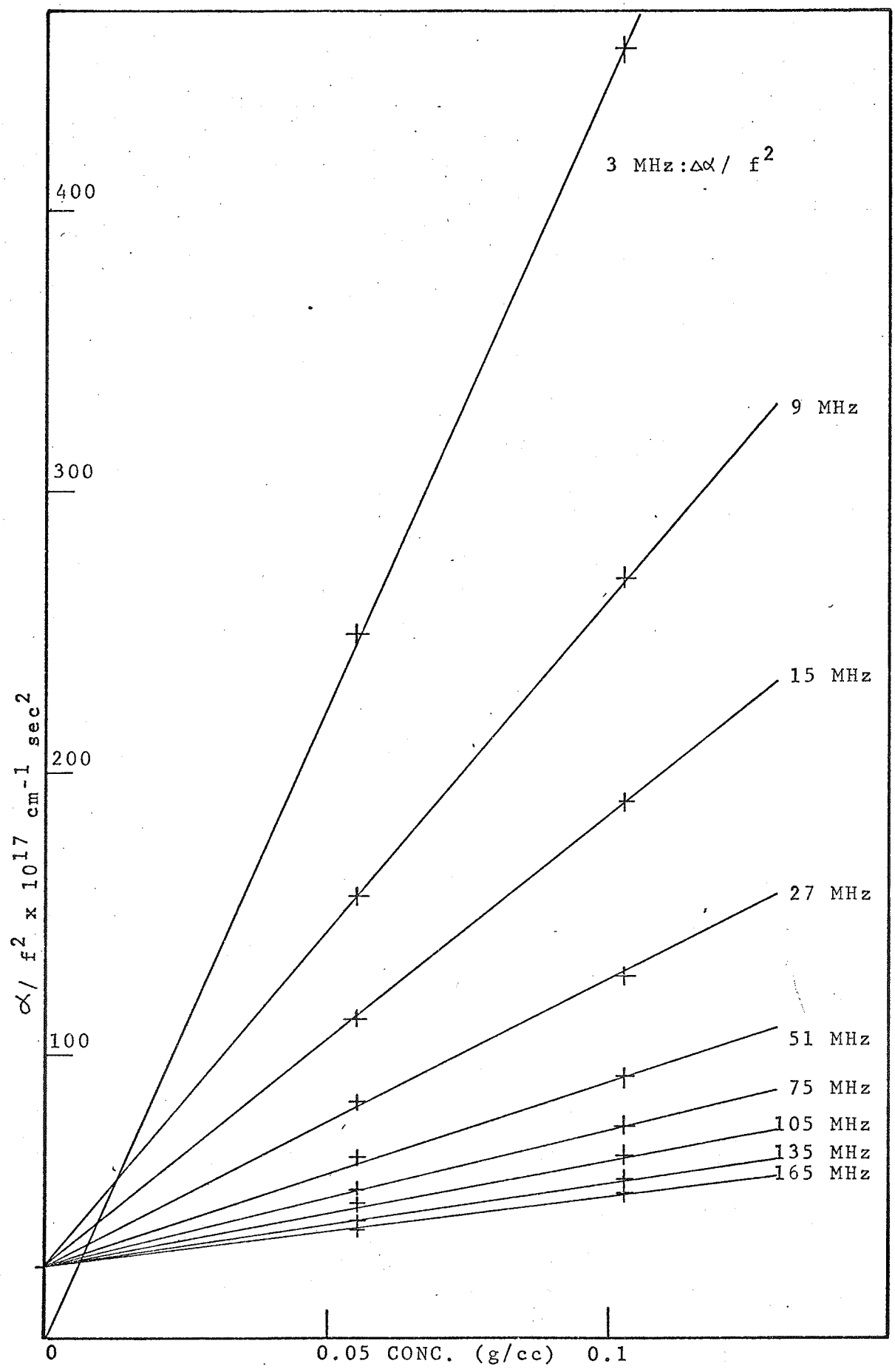


Figure 4-3 Absorption vs Concentration, Bovine Serum Albumin

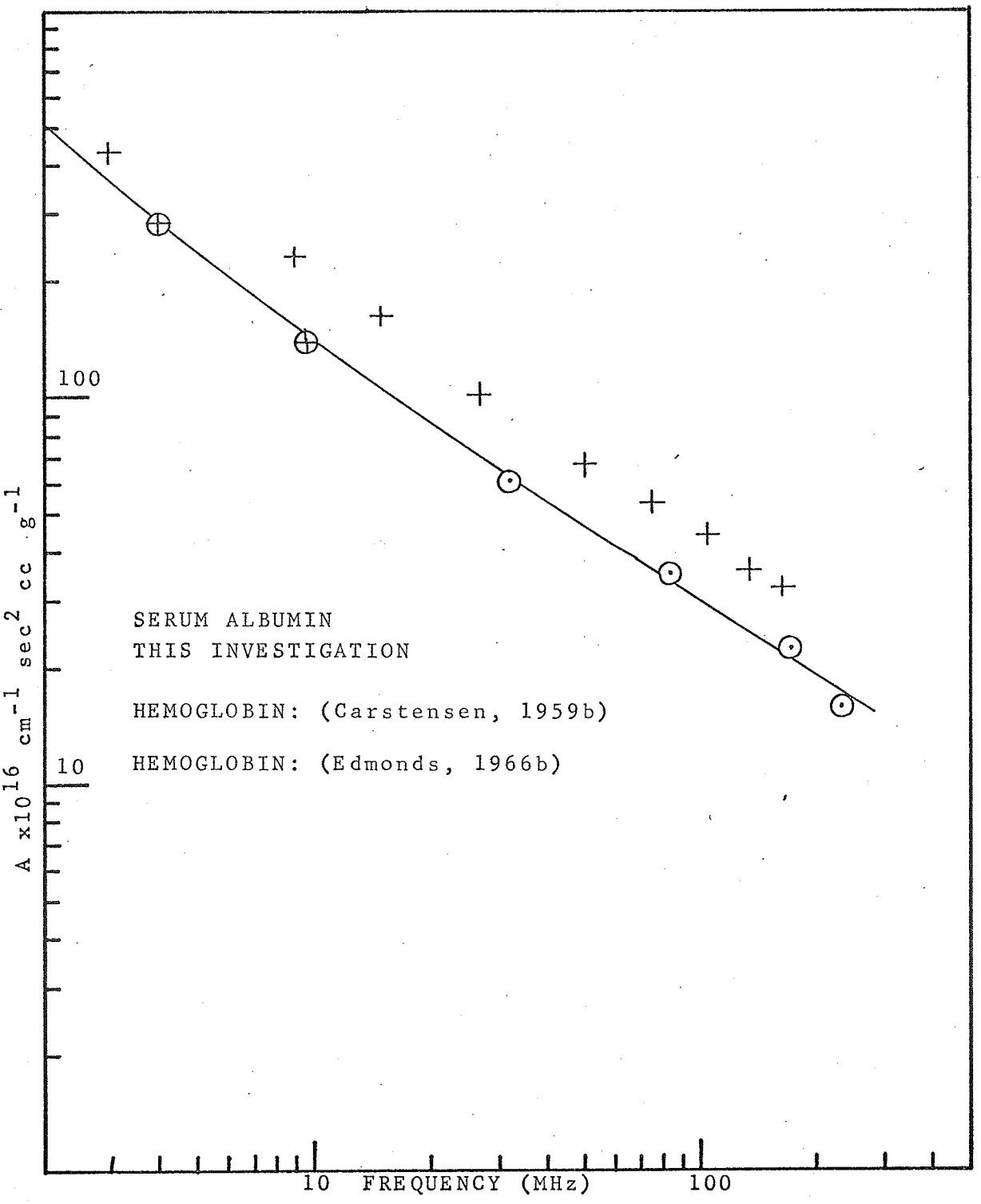


Figure 4-4: Bovine Serum Albumin

TABLE 4-1

Values of A for DEXTRAN and SERUM ALBUMIN

$A \times 10^{16}$ $cm^{-1}$ $sec^2$ $cc$ $g^{-1}$

$T = 20.0^{\circ}C$

| $M_w \times 10^{-3}$ | 11.2 | 21.8 | 39.8 | 72.0 | 167 | 370 | BSA |
|---|---|---|---|---|---|---|---|
| f(MHz) | | | | | | | |
| 3 | 122. | 143. | 147. | 147. | - | - | 430 |
| 9 | 74. | 75. | 77. | 73. | 71. | 68. | 235 |
| 15 | 55. | 57. | 56. | 56. | - | 51. | 163 |
| 27 | 41. | 38. | 38. | 40. | 37. | 39. | 102 |
| 39 | 29. | - | 30. | - | - | - | - |
| 45 | - | 28. | - | - | - | 25. | _ |
| 51 | 26. | 24. | 26. | 25. | - | - | 68 |
| 75 | 20. | 21. | 22. | 20. | 18. | 17. | 53 |
| 81 | - | - | 19. | - | - | - | - |
| 105 | - | - | - | 18. | - | - | 44 |
| 135 | - | 17. | - | 16. | - | 16. | 36 |
| 165 | - | 18. | - | 15.3 | - | 12.6 | 32 |
| 195 | - | 18 | - | - | - | 15.3 | - |

Underlined values occur at frequencies such that

$2 < \omega T_i < \frac{N^2}{250}$; see Appendix I.

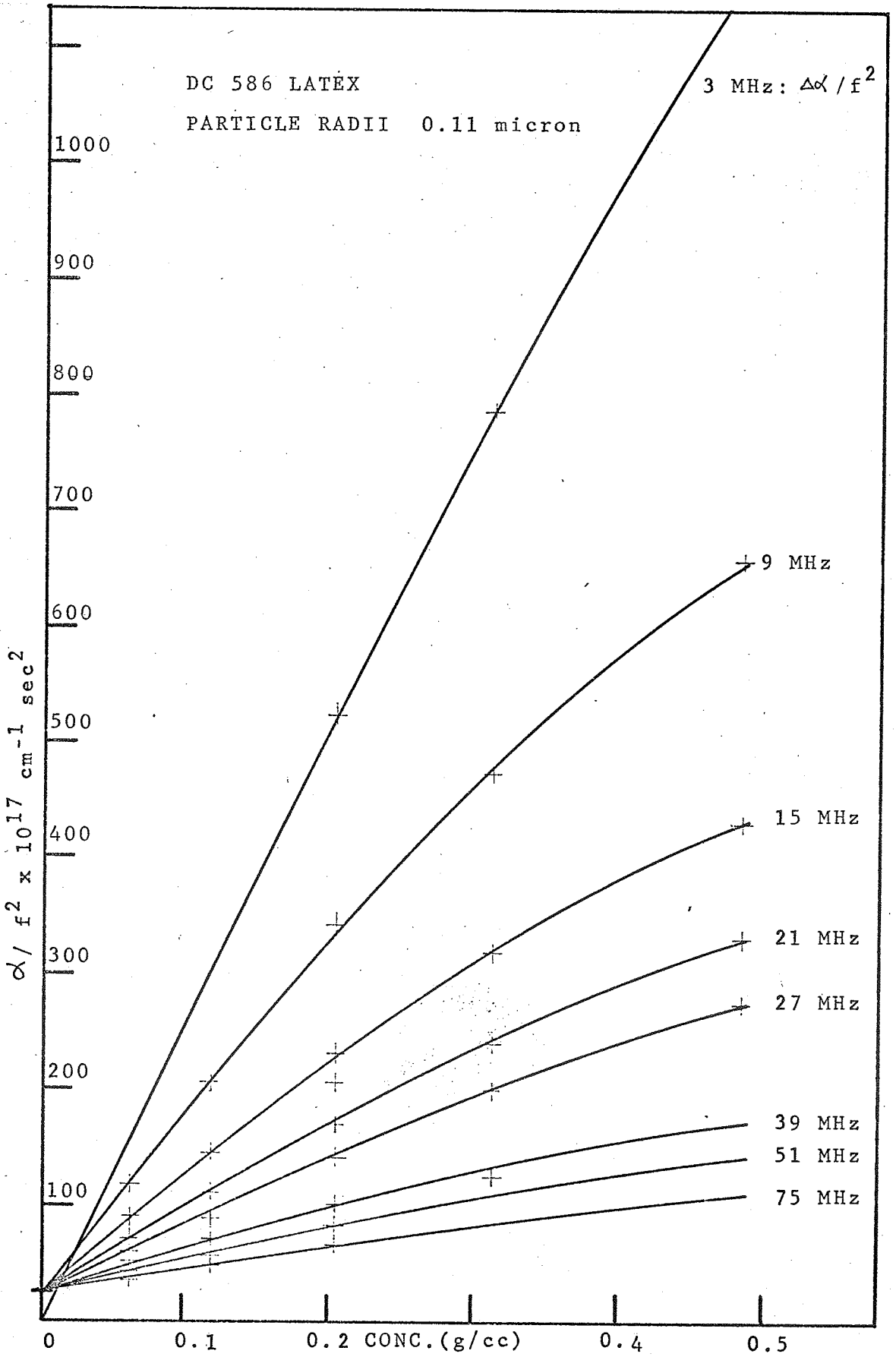


Figure 4-5 Absorption vs Concentration, DC 586 Latex

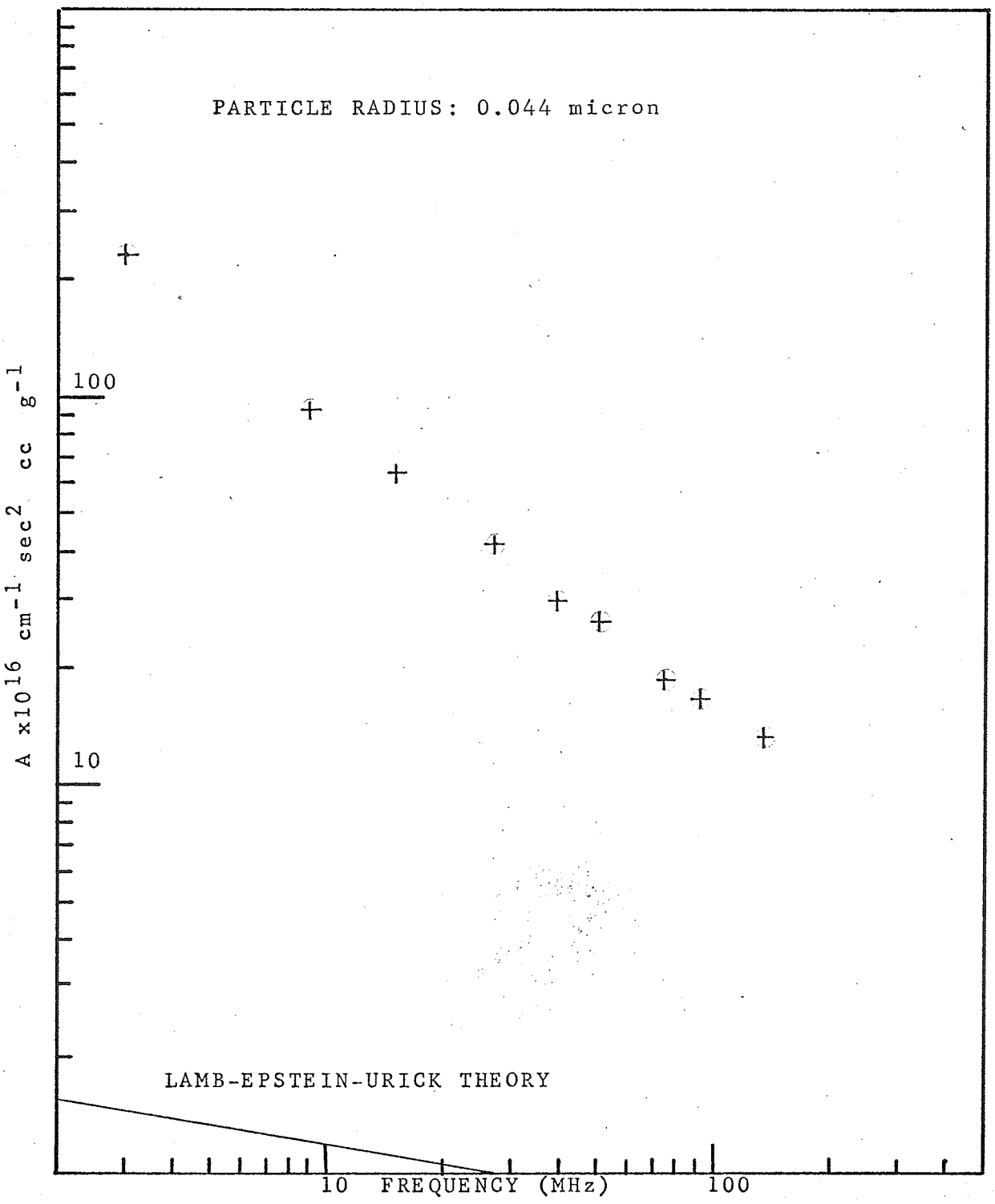


Figure 4-6: Particle Radius; 0.044 micron